



Horizon 2020 Societal challenge 5:  
Climate action, environment, resource  
efficiency and raw materials

## VERIFY

### Observation-based system for monitoring and verification of greenhouse gases

GA number 776810, RIA

<b>Deliverable number (relative in WP)</b>	D3.6
<b>Deliverable name:</b>	Final bottom-up model simulations
<b>WP / WP number:</b>	3
<b>Delivery due date:</b>	Month 41 (30/06/2021)
<b>Actual date of submission:</b>	Month 50 (07/03/2022)
<b>Dissemination level:</b>	Public
<b>Lead beneficiary:</b>	CEA
<b>Responsible</b>	Matthew McGrath
<b>Contributor(s):</b>	Sophia Walther, Raphael Ganzenmüller, Matthias Kuhnert, Matteo Vizzarri, Juraj Balkovic, Andrey Krasovskii, Bas Lerink, Sara Filipek, Mart-Jan Schelhaas, Gert-Jan Nabuurs, Meike Becker, Juergen Knaue, Frederic Chevallier, Philippe Ciais, Matthew McGrath
<b>Internal reviewer:</b>	Philippe Peylin

<b>Changes with respect to the DoA</b>
Delivery date was postponed from 31/05/2021 to end 2021 in agreement with the EC.
<b>Dissemination and uptake (Who will/could use this deliverable, within the project or outside the project?)</b>
The bottom-up simulation results are freely available (in some cases, registration is/will be necessary). The simulation results provide the initial guesses for top-down modeling approaches in WP3, in addition to be used in the synthesis product in WP5. The webpage for data download is listed later in this table.
<b>Short Summary of results (&lt;250 words)</b>
<p>Models play a crucial role in the quantification of GHG emissions. They can extrapolate and interpolate measurements spatially and temporally. Different models are designed for different purposes, from data-driven models that make the most efficient use of existing data, to process-based models which provide increased resolution of underlying driving mechanisms. VERIFY incorporates a wide variety of different model types to enable the pre-operational system to respond to a far-reaching host of questions.</p> <p>Therefore, the aim of this WP is to simulate terrestrial carbon fluxes from ecosystems, both natural and managed. Using harmonized input data collected and reported on in D3.3, WP3 produced a variety of gridded flux and stock estimates of carbon within Europe. This particular deliverable shows carbon dioxide emissions from croplands, grasslands, and forests across the continent, using a variety of approaches. These approaches include models making extensive use of country-level statistics; those aiming for comprehensive descriptions of ecosystem processes; and statistical upscaling of site-level results to the continental scale.</p> <p>This deliverable provides details about the results of the final round of simulations from the bottom-up land models. Simulation methods have been improved during the course of the project, reflecting new scientific and technical understanding. In addition, model results are available for several models not included in previous deliverables. This includes new types of fluxes, such as lateral transport of carbon and carbon dioxide fluxes from coastal ocean regions.</p>
<b>Evidence of accomplishment (report, manuscript, web-link, other)</b>
<p>All the simulation results will be accessible through the dedicated data THREDDS server: <a href="https://verifydb.lsce.ipsl.fr/thredds/catalog/verify/WP3/catalog.html">https://verifydb.lsce.ipsl.fr/thredds/catalog/verify/WP3/catalog.html</a></p> <p>Note that some of these data may be password protected during a consolidation phase and thus only accessible to the VERIFY partners (accessible through the internal share-point platform). To distinguish datasets submitted for this round of simulations, the identifier in the file name is changed from “V1” to “V3”, in addition to the submission date being generally later. Work is under consideration to change the naming scheme to use v2021 for clarity, but that needs to be carried out in cooperation with WP6.</p>

Version	Date	Description	Author (Organisation)
V0.1	19/06/21	Creation/Writing	Matthew McGrath (CEA)
V0.2	01/07/21 – 01/01/22	Writing/Formatting of methods and results	Sophia Walther (MPI-BGC), Raphael Ganzenmüller (LMU), Matthias Kuhnert (ABDN), Matteo Vizzarri (JRC), Juraj Balkovic (IIASA), Andrey Krasovskii (IIASA), Bas Lerink, Sara Filipek, Mart-Jan Schelhaas, Gert-Jan Nabuurs (WENR), Meike Becker (Bergen), Juergen Knauer (WSydney), Frederic Chevallier, Philippe Ciais, Matthew McGrath (CEA)
V1.0		Formatting/Delivery on the Participant Portal	Matthew McGrath, Philippe Peylin (CEA) and Géraud Moulas (ARTTIC)

<b>1. Glossary</b>	<b>5</b>
<b>2. Executive Summary</b>	<b>6</b>
<b>3. Introduction</b>	<b>7</b>
<b>4. Model descriptions</b>	<b>8</b>
4.1. BLUE	9
4.2. CABLE-POP	10
4.3. CBM-CFS3	12
4.4. Coastal ocean fluxes	17
4.5. ECOSSE	20
4.6. EFISCEN Space	22
4.7. EPIC-IIASA	23
4.8. Fluxcom	26
4.9. G4M+FLAM	27
4.10. Lateral fluxes	29
4.11. ORCHIDEE	30
<b>5. Model Results</b>	<b>31</b>
5.1. BLUE	31
5.2. CABLE-POP	32
5.3. CBM-CFS3	33
5.4. Coastal ocean fluxes	35
5.5. ECOSSE	35
5.6. EFISCEN Space	37
5.7. EPIC-IIASA	40
5.8. Fluxcom	41
5.9. G4M+FLAM	44
5.10. Lateral Fluxes	45
5.11. ORCHIDEE	45
<b>6. Conclusions</b>	<b>47</b>

# 1. Glossary

Abbreviation / Acronym	Description/meaning
<b>ABG</b>	Aboveground biomass
<b>BAU</b>	Business as usual
<b>CRF</b>	Common reporting framework
<b>DGVM</b>	Dynamic global vegetation model
<b>GPP</b>	Gross primary product
<b>KP</b>	Kyoto Protocol
<b>LULC</b>	Land use and land cover
<b>LULUCF</b>	Land use and land cover change
<b>NEP</b>	Net ecosystem productivity
<b>NPP</b>	Net primary productivity
<b>RS</b>	Remote sensing
<b>SOM</b>	Soil organic matter
<b>TRENDY</b>	A model intercomparison project using DGVMs to look the carbon cycle

## 2. Executive Summary

National greenhouse gas inventories often have very high uncertainties associated with carbon dioxide emissions and uptake from land use, land use change, and forestry (LULUCF) activities. This is due to a variety of reasons, many related to the fact that LULUCF activities occur on highly heterogeneous landscapes, where local conditions such as soil and micro-climates can dramatically impact the ability of plants to uptake and store carbon. In addition, LULUCF activities are spread across wide spatial areas which have traditionally been more difficult to monitor, as opposed to being point-sources of emissions like power plants. Finally, even classification of a parcel of land into a specific land use/land cover type is not always evident, which has led countries to use varying definitions of things like “forest”. These factors make it challenging to compare flux estimates from different reporting entities.

Over the years, a variety of approaches have developed to provide estimates of LULUCF emissions from ecosystems. These include data-driven approaches which make heavy use of national statistics ; process-based models which simulate realistic ecosystem dynamics, parameterized by observations; and statistical upscaling techniques which take detailed site-level measurements and create “wall-to-wall” estimates covering entire regions. In VERIFY, the WP3 challenge is to take all these different approaches and use them to reduce the uncertainty in LULUCF CO<sub>2</sub> emissions.

The goal of VERIFY WP3 is to run a harmonized model intercomparison using operational (i.e., up to the previous year) forcing data. Such a comparison is carried out on global scales for models of similar types (e.g., TRENDY), but much of the effort in WP3 is put into the best way to do this when the model structure and their approach to solving problems is different. For the final complete round of simulations in the project (2021), the work from 2020 was built-upon through the addition and refinement of the groups who submitted bottom-up results to WP3. This includes a new model, CABLE-POP, which is not officially a partner in VERIFY but who regularly submits results to TRENDY. This demonstrates growth potential of the VERIFY pre-operational system. In addition, further progress was made on using standardized input data (meteorological and nitrogen) to drive models, which greatly improves comparison of results. This effort, and the CO<sub>2</sub> fluxes from ecosystems submitted to WP3 summarized in this deliverable, are fundamental to the synthesis efforts in WP5, and the increased use of harmonized datasets represents an important step towards that goal.

### 3. Introduction

D3.6 summarizes the final complete round of the bottom-up simulations for the project VERIFY, consisting of carbon dioxide fluxes coming from various human and natural ecosystems across Europe. VERIFY takes a different approach to standard model intercomparison projects, where simulation inputs are harmonized across many incarnations of a single model class in order to provide more robust estimates of flux uncertainty due to model structure. Instead, VERIFY begins with a wide collection of bottom-up model classes all capable of predicting the carbon dioxide net biome production (i.e., the net flux of carbon dioxide from an ecosystem, taking into account disturbances like wood harvest) but only uses one or two examples of each class. In addition, sector-specific models are included, as these models often have much more detail than generally-applicable ecosystem models and can incorporate more observational data differentiating, for example, between tree species, crop varieties, and management practices. This provides the potential for more realistic constraints on the fluxes and better incorporation of heterogeneous data.

D3.6, like its predecessors D3.4 and D3.5, is intricately related to other WPs in support of the overall VERIFY objective of advancing the development of accurate and robust observation-based methods for quantifying GHG emissions and sinks, in particular by providing a portfolio of synthesis products for land-based carbon dioxide emission in Europe. In this way, WP3 bottom-up simulations complement the high-resolution bottom-up fossil fuel and biofuel emission estimates of CO<sub>2</sub> produced in WP2, providing a complete picture of carbon dioxide emissions from the European land surface. Emissions and absorption of other strong greenhouse gases, notably methane and nitrous oxide, are covered in WP4, thus covering three gaseous species known to be highly important to climate processes. Results from bottom-up models such as those presented in this deliverable can serve as initial guesses for top-down approaches reported from WP3 in other deliverables. Results highlighted in D3.6 will be merged with the rest of the project methods in the synthesis prepared in WP5 (as was done for D3.4 and D3.5), and when compared against inventory results from WP1, can help identify common language between inventory-taking in accordance with IPCC guidelines and cutting-edge scientific results.

This deliverable is divided into sections for all bottom-up models which submitted results to WP3 this year. This is a departure from previous deliverables who included models expected to provide results to WP3 at some point during the VERIFY project. The first major section describes the models themselves, including updates made this year, while the second focuses on results achieved this year. One change to D3.6 compared to D3.4 and D3.5 is that “Changes for next year” are no longer included in the description of the models, as this is the final year of the project.

## 4. Model descriptions

**Table 1 : Models providing bottom-up carbon fluxes in the context of VERIFY.**

Name/ model	Inst.	Spatial Coverage	Sector	Temporal Resolution	Time frame	Contact in the project
<b>BLUE</b>	LMU	Europe, 0.01° and 0.25° degree	Land cover change	Annual	1960- 2019	Raphael Ganzenmüller <sup>a</sup>
<b>CABLE-POP</b>	U Western Sydney	Europe (35N:73N, 25W:45E), 0.125 degrees	Forest, grasslands, croplands	1M	1970- 2020	Juergen Knauer <sup>b</sup>
<b>CBM-CFS3</b>	JRC	Country totals, EU- 25+UK	Forests	Annual	2000- 2015 ; 2020	Matteo Vizzarri <sup>c</sup>
<b>Coastal_fluxes_RF_v2021.2</b>	UiB	Europe (33N:84N, 15W:35E)	Marine CO2 fluxes	monthly	1998- 2020	Meike Becker <sup>d</sup>
<b>ECOSSE</b>	ECOSSE	UNIABDN	Europe (35N:73N, 25W:45E)	Grasslands, croplands	1981- -2020	Matthias Kuhnert <sup>e</sup>
<b>EFISCEN-Space</b>	WUR	Europe (35N:73N, 25W:45E)	Forests	Single value	Taken as the mean from 2005- 2020	Mart-Jan Schelhaas <sup>f</sup>
<b>EPIC-IIASA</b>	IIASA	1x1 km EU-33	cropland, grassland	1M	1981- 2020	Juraj Balkovič <sup>g</sup>
<b>Fluxcom</b>	MPI- BGC	Europe (35N:73N, 25W:45E)	All	hourly	2002- 2020	Sophia Walther <sup>h</sup>
<b>G4M/FLAM</b>	IIASA	5 arc min	Forest	1M	2010- 2020	Andrey Krasovskiy <sup>i</sup>
<b>Lateral fluxes</b>	LSCE	Global, 0.083 degrees	Croplands, forests, rivers, lakes	1Y	1961- 2019	Frederic Chevallier <sup>j</sup>
<b>ORCHIDEE</b>	LSCE	Europe	Forest,	1M	1970-	Matthew

		(35N:73N, 25W:45E), 0.125 degrees	grasslands, croplands		2020	McGrath <sup>k</sup>
--	--	--	--------------------------	--	------	----------------------

**Email addresses of contact persons:**

<sup>a</sup> [raphael.ganzenmueller@geographie.uni-muenchen.de](mailto:raphael.ganzenmueller@geographie.uni-muenchen.de)

<sup>b</sup> [J.Knauer@westernsydney.edu.au](mailto:J.Knauer@westernsydney.edu.au)

<sup>c</sup> [matteo.vizzarri@ec.europa.eu](mailto:matteo.vizzarri@ec.europa.eu)

<sup>d</sup> [Meike.becker@uib.no](mailto:Meike.becker@uib.no)

<sup>e</sup> [Matthias.kuhnert@abdn.ac.uk](mailto:Matthias.kuhnert@abdn.ac.uk)

<sup>f</sup> [martjan.schelhaas@wur.nl](mailto:martjan.schelhaas@wur.nl)

<sup>g</sup> [balkovic@iiasa.ac.at](mailto:balkovic@iiasa.ac.at)

<sup>h</sup> [swalth@bgc-jena.mpg.de](mailto:swalth@bgc-jena.mpg.de)

<sup>i</sup> [krasov@iiasa.ac.at](mailto:krasov@iiasa.ac.at)

<sup>j</sup> [frederic.chevallier@lsce.ipsl.fr](mailto:frederic.chevallier@lsce.ipsl.fr)

<sup>k</sup> [matthew.mcgrath@lsce.ipsl.fr](mailto:matthew.mcgrath@lsce.ipsl.fr)

**Table 2 : Use of forcing data provided by the VERIFY project in models providing bottom-up carbon fluxes.**

Name/ model	Estimate of net biome productivity (NPP-HR- disturbances)?	Use VERIFY meteorological forcing (CRUHAR/CRUE RA)?	Use VERIFY land use/land cover change forcing (Hilda+)?	Use VERIFY nitrogen forcing?
<b>BLUE</b>	No	No	Yes	No
<b>CABLE-POP</b>	Yes	Yes	Partially (see Methods)	No
<b>CBM-CFS3</b>	Yes	No	No	No
<b>Coastal_fluxes_ RF_v2021.2</b>	No	No	No	No
<b>ECOSSE</b>	Yes	Yes	Yes	No
<b>EFISCEN-Space</b>	Yes	No	No	No
<b>EPIC-IIASA</b>	Yes	Yes	No	No
<b>Fluxcom</b>	No	Yes	Yes	No
<b>G4M/FLAM</b>	No (only NPP)	Yes	Yes	No
<b>Lateral fluxes</b>	Yes	No	No	No
<b>ORCHIDEE</b>	Yes	Yes	Yes	Yes

## 4.1. BLUE

### 4.1.1. Model Description

BLUE is a bookkeeping model that provides an estimate of the net land use change carbon flux (Hansis et al., 2015). Transformation of natural vegetation to agriculture (cropland, pasture) and back, including gross transitions at the sub-grid scale (“shifting cultivation”) are considered, as well as wood harvesting. It is one of three bookkeeping models used in the Global Carbon Project’s annual carbon budget for estimating land use change emissions (Friedlingstein et al., 2020).

Within the VERIFY project, the underlying LULCC dataset of BLUE has been updated to HILDA+ (Winkler et al., 2021). HILDA+ is a global high-resolution dataset based on FAO, ESA CCI and other data streams and reports land cover classes and transitions in a binary classification scheme. In VERIFY, HILDA+ is adapted for the European domain. Since HILDA+ does not provide estimates of wood harvesting, we adjusted the harvest areas from LUH2 (Hurtt et al., 2020) to match HILDA+ forest and shrubland areas for consistency reasons. These improvements and additional changes in the model setup enable us now to run the model at a resolution of  $\sim 0.01^\circ$  (original res. of HILDA+), compared to previously  $\sim 0.25^\circ$  (original res. of LUH2). With the higher resolution emission sinks and sources can be detected more precisely than reported by any other ELUC emission model to date.

#### 4.1.2. References/link

P. Friedlingstein, M. O'Sullivan, M. Jones, et al. (2020). Global carbon budget 2020. *Earth System Science Data*, 12(4), 3269-3340.

E. Hansis, S. J. Davis, and J. Pongratz, J. (2015). Relevance of methodological choices for accounting of land use change carbon fluxes. *Global Biogeochemical Cycles*, 29(8), 1230-1246.

G. C. Hurtt, L. Chini, R. Sahajpal, et al. (2020). Harmonization of global land use change and management for the period 850–2100 (LUH2) for CMIP6. *Geoscientific Model Development*, 13(11), 5425-5464.

K. Winkler, R. Fuchs, M. Rounsevell, et al. (2021). Global land use changes are four times greater than previously estimated. *Nature communications*, 12(1), 1-10.

### 4.2. CABLE-POP

#### 4.2.1. Model Description

CABLE-POP (Haverd *et al.*, 2018) is a global terrestrial biosphere model and consists of a biogeophysics module (Wang & Leuning, 1998), a biogeochemistry module including cycles of nitrogen and phosphorus (Wang *et al.*, 2010) and modules simulating woody demography (Haverd *et al.*, 2013) as well as land use change and land management (Haverd *et al.*, 2018). CABLE-POP does not simulate dynamic vegetation and the distribution and cover fraction of PFTs is only affected by land use change. Only nitrogen and not phosphorus cycling was activated for the present simulations.

Two simulations were conducted for the VERIFY MIP: S0 (control, no changes in external forcing) and S3 (observed changes in atmospheric CO<sub>2</sub> concentration, N deposition, meteorology, and LUC) using an identical spinup for both S0 and S3. The following lists gives details on the input data used:

- Atmospheric CO<sub>2</sub>: same as for TRENDYv10
- N deposition: same as for TRENDYv10, regridded to 0.125° using conservative remapping

- Meteorology: as provided. Spinup and S0: Recycled from 1901-1920
- LUC: LUC from LUH2 data as used in TRENDYv10, but regridded from 0.25° to 0.125° using conservative remapping. However, a new baseline PFT map was created from the HILDA+ dataset (year 1901) to better capture the distribution of different vegetation types over Europe, i.e., the baseline PFT map comes from HILDA+, but all land-use transitions as well as management fluxes come from LUH2.

**Land use change:** Every grid cell in CABLE-POP consists of 1-3 **land use types**: primary forest, secondary forest, and grassland (one or two of them may be absent depending on the grid cell). Each land use type is again associated with a certain **plant functional type (PFT)** (i.e., forest can be evergreen needleleaf, evergreen broadleaf, etc.; grassland can be C3 or C4 grasses). The output is given on a PFT-basis (and given in units per m<sup>2</sup> PFT, not grid cell), and land use types are not considered in the output as provided to the VERIFY project. CABLE-POP simulates the four following transitions: primary forest to secondary forest, primary forest to grassland, secondary forest to grassland, grassland to secondary forest. CABLE-POP does not simulate croplands explicitly but does account for cropland harvest fluxes in the grassland land-use type. That means that the PFT “C3 grassland” comprises the land use types grasslands as well as crops. The two are completely identical in the absence of management (i.e., runs S0-S2) and differ only in the S3 runs, where a certain fraction of biomass (higher in crops than in grasslands) is removed every year. This fraction of biomass removal (harvest of agricultural products) is different for crops and grasslands. The fraction of crops vs. grasslands for each “C3 grassland” PFT comes from the LUH2 dataset.

#### 4.2.2. References/link

V. Haverd, B. Smith, G. D. Cook, et al. (2013). A stand-alone tree demography and landscape structure module for Earth system models. *Geophysical Research Letters* 40(19): 5234-5239.

V. Haverd, B. Smith, L. Nieradzic, et al. (2018). A new version of the CABLE land surface model (Subversion revision r4601) incorporating land use and land cover change, woody vegetation demography, and a novel optimisation-based approach to plant coordination of photosynthesis. *Geoscientific Model Development* 11(7): 2995-3026.

Y.-P. Wang, R. Leuning (1998). A two-leaf model for canopy conductance, photosynthesis and partitioning of available energy I: Model description and comparison with a multi-layered model. *Agricultural and Forest Meteorology* 91(1): 89-111.

Y.-P. Wang, R. M. Law, B. Pak (2010). A global model of carbon, nitrogen and phosphorus cycles for the terrestrial biosphere. *Biogeosciences* 7(7): 2261-2282.

## 4.3. CBM-CFS3

### 4.3.1. Model Description

The Carbon Budget Model developed by the Canadian Forest Service (CBM-CFS3, hereafter CBM) can simulate the historical and future stand- and landscape-level C dynamics of forests under different scenarios of harvest and natural disturbances (fires, storms), according to the standards described by the IPCC. Since 2009, CBM has been tested and validated by the JRC, and adapted to the European forest conditions. It is currently applied to 25 EU member states and the UK, both at the country and NUTS2 level.

Based on the model framework, each stand is described by area, age, land classes, and up to 10 classifiers based on administrative and ecological information and on silvicultural parameters (such as forest composition and management strategy). A set of yield tables defines the merchantable volume production for each species/forest type while species-specific allometric equations convert merchantable volume production into aboveground biomass at the stand level. For the initial year and any subsequent time step the model provides data on the net primary production (NPP), C stocks and fluxes as the annual C transfers between pools and to the forest product sector. With additional processing of the outputs, it can provide forestry-related indicators (e.g., standing volume and net annual increment of the standing volume).

The model can support policy anticipation, formulation and evaluation under the LULUCF (Land Use, Land Use Change and Forest) sector, and it is used to estimate current and future forest C dynamics, both as a verification tool (i.e., to compare the results with the estimates provided by other models) and to support EU legislation on the LULUCF sector (Grassi et al. 2018). In the biomass sector, CBM can be used in combination with other models to estimate the maximum wood harvest potential and the forest C dynamics under different assumptions of harvest and land use change (Jonsson et al., 2018).

CBM follows the IPCC reporting method 1 (Penman et al. 2003). The spatial framework coincides with the geographically referenced spatial units (SPUs) as relevant from the national forest inventories perspective. Each SPU can be identified with a forest stand characterized by tree species composition (i.e., forest type, FT), area, age, and other information, such as correspondence with appropriate yield curves, the forest management system and management type (MT), and main wood use, i.e., solid and energy (which can be derived from model outcomes). National forest inventories (e.g., statistical sampling NFIs or stand-wise forest inventories) are the key data sources. In a few cases, due to the lack of country-specific information, some input parameters are obtained from literature or values reported by other countries under similar conditions (e.g., biogeographical region). Other relevant parameters are provided by Pilli et al. (2018). Table 3 summarizes the main characteristics of the modelling exercise.

**Table 3 : main characteristics of CBM-CFS3 simulations for VERIFY**

Spatial coverage	Time coverage for input data (NFIs)	Time step 0 (initial year of simulation)	Total forest land area (year=1990) (ha·10 <sup>6</sup> )	Considered natural events	Land use change	Main outcomes
EU 25 Member States (excl. Cyprus and Malta) and UK [NUTS 0; NUTS 3]	1992-2010	1992-2000	138 [0.1-22.6]	Fire (10 cases); storm and sleet (16 cases); insect attacks (2 cases)	Afforestation; deforestation	NBP; C fluxes by pool

NFI standing volume and net annual increment data were used to build species-specific growth curves, combined with stand-level equations to convert merchantable volume per hectare into aboveground biomass, and partitioned into merchantable stem wood, other wood components (stump, tops, branches, sub-merchantable size trees), foliage components (Pilli et al. 2013; Pilli et al. 2016a) and belowground biomass. The impact of natural disturbances such as storms, sleet, fires and bark beetle attacks was also assessed (for background assumptions, please refer to Pilli et al. 2016a; 2016b). To define the decomposition rates of the DOM pools, 60 climatic units (CLUs) were created and associated with specific portions of country-level forest lands, based on a combination temperature, precipitation, and CORINE land cover datasets (see Pilli, 2012 for further details).

In terms of outputs, CBM provides annual estimates of C stocks and fluxes, such as the annual C transfers between pools, from pools to the atmosphere and from forest pools to the forest product sector, as well as ecological indicators such as the net primary production (*NPP*), heterotrophic respiration ( $R_h$ ) and net biome production (*NBP*). These variables (which represent only a few of those available) were calculated as follows (see also Kurz et al. 2009):

$$NPP = GPP - R_a \text{ [eq. 1]}$$

where: *NPP* is the net primary productivity, i.e., inputs of C from the atmosphere to the forest ecosystem; *GPP* is the carbon assimilated by plants during photosynthesis;  $R_a$  is the carbon released by plants through autotrophic respiration.

$$NEP = NPP - R_h \text{ [eq. 2]}$$

where: *NEP* is the net ecosystem productivity; *NPP* is the net primary production (see above);  $R_h$  is the heterotrophic respiration (i.e., decomposition).

$$NBP = NEP - H - D \text{ [eq. 3]}$$

where: *NBP* is the net biome productivity; *H* represents the direct biomass losses due to harvest; *D* represents the direct losses due to natural disturbances (e.g., fires).

Once the harvest demand was defined (BaU scenario), we applied CBM to (i) check if it is possible to harvest that amount for the period 2000 – 2015 and (ii) simulate the forest development under that harvest level from 2016 to 2030. The historical harvest (2000-2015) was inferred for each country from the amount of roundwood removals reported by FAOSTAT, further distinguishing between industrial roundwood and fuelwood. If needed, data on harvest were also compared, and possibly corrected, with other information from the literature (Pilli et al., 2015).

Land use change (i.e., afforestation and deforestation) was also taken into account. To be consistent with other studies, 1990 was used as the base year (see details in Pilli et al., 2016a). Afforestation was modelled through country-specific model runs, always beginning in 1990, and applying the historical annual rate of afforestation/reforestation reported by each country up to 2012 (Pilli et al., 2016b). The total amount of afforestation/reforestation per year was distributed between different forest types (FTs), according to the proportional amount of the forest management area. Deforestation was modelled by decreasing the forest area since the base year (=1990) until the time step 0 (when simulation starts), according to the total amount of forest area losses as reported by the countries (KP CRF tables, 2014).

For further details on the methodology, please refer to Pilli et al. (2017) and Grassi et al. (2018).

Compared to previous report, we made the following improvements:

- update of input data for harvest: 2000-2015 values based on historical management practices, and 2016-2020 based on the continuation of historical management practices, as defined within the period 2000 - 2015 (Business as Usual pathway, as defined in Grassi et al., 2018)
- revision of methodological assumptions within the CBM modelling framework, in particular concerning the Archive Index Database for EU Member States and the UK (see Pilli et al. 2018)

Such improvements represent a first stage of an ongoing effort to further develop CBM as a spatially-explicit model architecture and to include the expected impact of climate change within long-term model runs. This activity has recently started with the distribution of model runs across Climate Units (land classification system based on different combinations of average precipitation and temperature) (see Figure 1 below) accompanied by the incorporation of climate parameters varying the potential forest growth during the simulations (see Pilli et al. 2018 for more details).

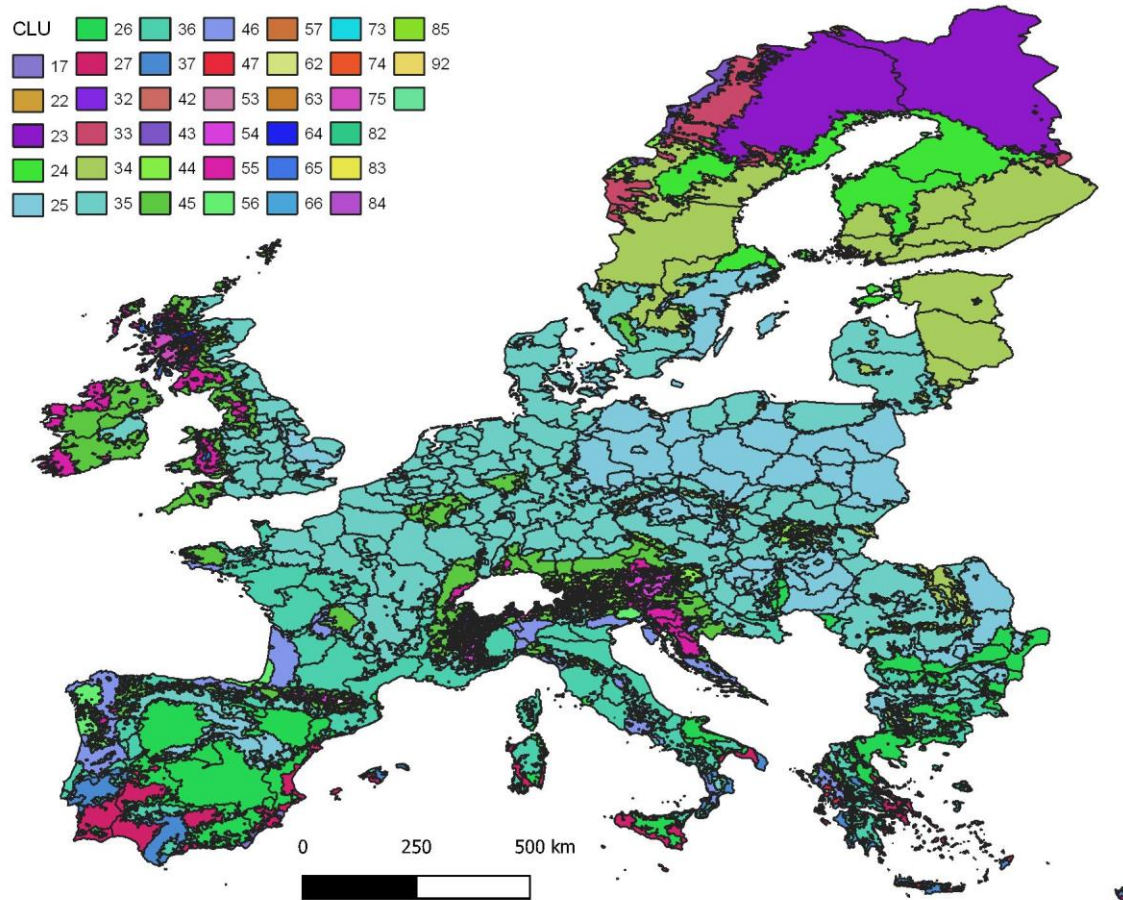


Figure 1 : Climatic Units (CLUs) of EU 25 + UK based on mean annual temperatures (°C) and total annual precipitations (mm). For codes, please refer to <https://data.jrc.ec.europa.eu/dataset/jrc-cbm-eu-aidb#dataaccess> > Main Tables modified in the EU AIDB > Ecological Boundaries.

#### 4.3.2. References/link

FAOSTAT: <http://www.fao.org/faostat/en/#data/FO> (last access: January 2016), 2013.

G. Grassi, R. Pilli, J. House, et al. (2018). Science-based approach for credible accounting of mitigation in managed forests. *Carbon Balance Manage* 13, 8. <https://doi.org/10.1186/s13021-018-0096-2>

R. Jonsson, V. Blujdea, G. Fiorese, et al. (2018). Outlook of the European forest-based sector: forest growth, harvest demand, wood-product markets, and forest carbon dynamics implications. *iForest - Biogeosciences and Forestry*, 11(2), 315–328. doi:10.3832/ifor2636-011

KP CRF Tables: Submission 2014, [http://unfccc.int/national\\_reports/annex\\_i\\_ghg\\_inventories/national\\_inventories\\_submissions/items/7383.php](http://unfccc.int/national_reports/annex_i_ghg_inventories/national_inventories_submissions/items/7383.php) (last access: June 2014), 2014.

W. A. Kurz, C. C. Dymond, T. M. White, et al. (2009). CBM-CFS3: A model of carbon-dynamics in forestry and land-use change implementing IPCC standards. *Ecological Modelling*, 220(4), 480–504. doi:10.1016/j.ecolmodel.2008.10.018

J. Penman, M. Gytarsky, T. Hiraishi, et al (Eds.). (2003). *Good Practice Guidance for Land Use, Land-Use Change and Forestry*. IPCC, Intergovernmental Panel on Climate Change, Institute for Global Environmental Strategies for the Intergovernmental Panel on Climate Change, Hayama, Kanagawa, Japan.

R. Pilli, G. Fiorese, G., Grassi, et al. (2016a). LULUCF contribution to the 2030 EU climate and energy policy, EUR 28025, Luxembourg, Publication Office of the European Union, doi:10.2788/01911, 2016b.

R. Pilli, G. Grassi, W. A. Kurz, et al. (2016b). Modelling forest carbon stock changes as affected by harvest and natural disturbances. I. Comparison with countries' estimates for forest management. *Carbon Balance and Management* 11: 5. doi:https://doi.org/10.1186/s13021-016-0047-8.

R. Pilli, G. Grassi, G., W. A. Kurz, et al. (2017). The European forest sector: past and future carbon budget and fluxes under different management scenarios, *Biogeosciences*, 14, 2387–2405, https://doi.org/10.5194/bg-14-2387-2017.

R. Pilli, G. Grassi, W. A. Kurz, et al. (2016c). Modelling forest carbon stock changes as affected by harvest and natural disturbances. II. EU-level analysis. *Carbon Balance and Management*, 11(1). doi:10.1186/s13021-016-0059-4

R. Pilli, S. Kull, V. Blujdea, et al. (2018). The Carbon Budget Model of the Canadian Forest Sector (CBM-CFS3): customization of the Archive Index Database for European Union countries, *ANNALS OF FOREST SCIENCE*, ISSN 1286-4560 (online), 75, p. 71, JRC107719.

R. Pilli, R. Alkama, A. Cescatti, et al. (in prep). The European forest carbon budget under future climate conditions and current management practices.

R. Pilli. (2012). Calibrating CORINE Land Cover 2000 on forest inventories and climatic data: An example for Italy, *Int. J. Appl. Earth Obs.*, 19, 59–71, doi:10.1016/j.jag.2012.04.016, 2012.

## 4.4. Coastal ocean fluxes

### 4.4.1. Model Description

Coastal\_Fluxes\_RF\_v2021.2 provides air-sea CO<sub>2</sub> fluxes and seawater pCO<sub>2</sub> in European shelf seas, covering the area from the western Mediterranean to the Barents Sea. The pCO<sub>2</sub> maps were generated applying a random forest regression routine on a gridded fCO<sub>2</sub> observations from SOCAT (Bakker et al., 2016) combined with a set of driver data (for example sea surface temperature, mixed layer depth or chlorophyll concentration). The fluxes were calculated from these pCO<sub>2</sub> maps combined with the atmospheric xCO<sub>2</sub> in the marine boundary layer and 6-hourly wind speed data. For the adjacent open ocean region, Coastal\_Fluxes\_RF\_v2.1 was merged with the CarboScope CO<sub>2</sub> fluxes (Rödenbeck et al, 2013).

Due to the large oceanographic and biogeochemical variability of the European shelf seas, the region was divided into a set of seven subregions for the pCO<sub>2</sub> mapping routine (Figure 2). We defined data to be coastal if they were obtained in regions with water depth of less than 500 m water or within 100 km from shore. We extracted available fCO<sub>2</sub> observations on the European shelf from the SOCAT (Bakker et al., 2016) database ([www.socat.info](http://www.socat.info), version 2021, quality flags A-E) and gridded these data on a monthly 0.125° x 0.125° grid. The driver data used for the fitting routines are listed in Table 4; these are supplied as 3D mapped distributions (lat x lon x time). For establishing the statistical fits, driver data were regridded on the same grid as the pCO<sub>2</sub> data.

We use a bagged regression tree model for the random forest fits (Belgiu and Drăguț, 2016). The tree is built by splitting the input data into subsets, based on the characteristics of the driver data. We used 500 independent regression trees, each based on a random subset of the input data. The leaf size (i.e., the size at which a subset is not divided any further) was chosen to be 20. This is a compromise, as reducing the leaf size results in a better description of the input data (low in-sample RMSE) but also increases the risk risk of overfitting. The output of these trees was averaged to obtain the final model response. Results of the fitting are shown in

Table 5.

**Table 4 : Products used as driver data in the pCO<sub>2</sub> mapping routine and for calculating the fluxes**

Product used	Resolution	Reference
<b>fCO<sub>2</sub> observations</b>		SOCAT dataset (Bakker et al., 2016)
<b>Chl <i>a</i></b>	4 km x 4 km, monthly	Global Ocean Chlorophyll II (Copernicus-GlobColour) from Satellite Observations - Reprocessed
<b>MLD/SST/SSS</b>	0.25° x 0.25°, monthly	(Guinehut et al., 2012)

<b>BATHYMETRY</b>	2 min x 2min	(National Geophysical Data Center, 2006)
<b>ICE</b>	0.25° x 0.25°, monthly	(Cavalieri et al., 1996)
<b>xCO<sub>2</sub>, atmosphere</b>	10 zonal, latitudinal bands, monthly	NOAA Greenhouse Gas Marine Boundary Layer Reference
<b>Rödenbeck pCO<sub>2</sub>, version oc_v2021</b>	5° x 4°, daily	(Rödenbeck et al., 2013)
<b>Wind speed, air pressure</b>	6-hourly	(Kanamitsu et al., 2002)

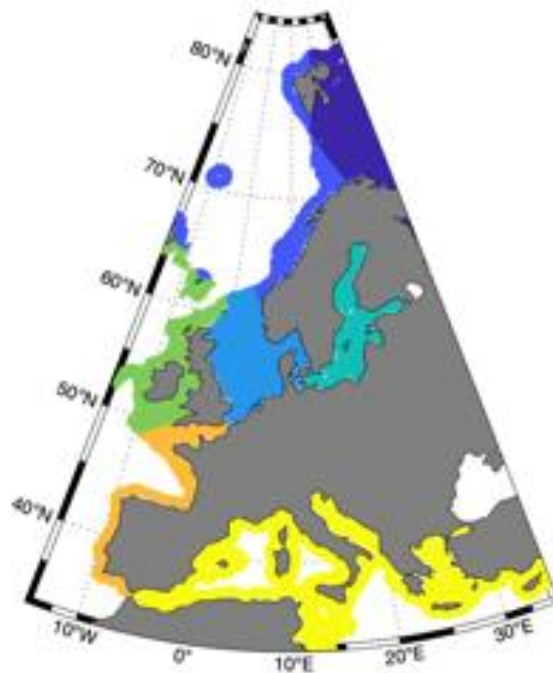


Figure 2 : Overview over the study area and the seven different subregions

Table 5 : RMSE and R2 of the Random Forest pCO<sub>2</sub> mapping routine

	RMSE	R <sup>2</sup>
Barents Sea	9.9	0.93
Norwegian Coast	15.6	0.89
North Sea	19.0	0.85
Baltic Sea	33.5	0.92
Celtic Sea/Icelandic and Irish coasts	15.5	0.84
English Channel/French and Portuguese Coasts	20.2	0.81
Mediterranean	11.4	0.95

The air-sea disequilibrium was calculated as the difference between our mapped  $f\text{CO}_2$  values and the atmospheric  $f\text{CO}_2$  in each grid cell and time step. The atmospheric  $f\text{CO}_2$  was determined by converting the  $x\text{CO}_2$  from the NOAA Marine Boundary Layer Reference product from the NOAA GMD Carbon Cycle Group into  $f\text{CO}_2$  by using the monthly SST and SSS data (Table 4) and monthly air pressure data from the NCEP-DOE Reanalysis 2. We calculated the air-sea  $\text{CO}_2$  flux ( $F$ ) according to Equation 1, such that negative fluxes enter into the ocean. The gas transfer velocity,  $k$ , was determined using the quadratic wind speed ( $u$ ) dependency of (Wanninkhof, 2014) (Equation 2). The Schmidt number,  $Sc$ , was calculated according to (Wanninkhof, 2014) and the solubility coefficient for  $\text{CO}_2$ ,  $K_0$ , after (Weiss, 1974).

$$F = k \cdot K_0 \cdot (f\text{CO}_{2,\text{sw}} - f\text{CO}_{2,\text{atm}}) \quad (1)$$

$$k = a_q \cdot \langle u^2 \rangle \cdot \left( \frac{Sc}{660} \right)^{-0.5} \quad (2)$$

In our calculations, we used 6-hourly winds of the NCEP-DOE Reanalysis 2 product. The coefficient  $a_q$  in Equation 2 is strongly dependent on the wind product used. We determined it to be  $a_q = 0.16 \text{ cm h}^{-1}$  for the 6-hourly NCEP 2 product following the recommendations of (Naegler, 2009) and by using the World Ocean Atlas sea surface temperatures (Locarnini et al., 2018). For the monthly product the monthly mean of the second moment of the NCEP2 6-hourly wind speeds was used to determine  $k$ . As the gas exchange in areas that are considered 100% ice covered from satellite images should not be completely neglected, we used a sea ice barrier effect for a 99% sea ice cover in all grid cells where the sea ice coverage exceeded 99%.

#### 4.4.2. References/link

D. C. E. Bakker, B. Pfeil, C. S. Landa, et al. 2016. A multi-decade record of high-quality  $f\text{CO}_2$  data in version 3 of the Surface Ocean  $\text{CO}_2$  Atlas (SOCAT). *Earth System Science Data* 8, 383–413. <https://doi.org/10.5194/essd-8-383-2016>

M. Belgiu, L. Drăguț. 2016. Random forest in remote sensing: A review of applications and future directions. *ISPRS Journal of Photogrammetry and Remote Sensing* 114, 24–31. <https://doi.org/10.1016/j.isprsjprs.2016.01.011>

D. J. Cavalieri, C. L. Parkinson, P. Gloersen, et al. 1996. Sea Ice Concentrations from Nimbus-7 SMMR and DMSP SSM/I-SSMIS Passive Microwave Data, Version 1, Monthly.

S. Guinehut, A.-L. Dhomp, G. Larnicol, et al. 2012. High resolution 3-D temperature and salinity fields derived from in situ and satellite observations. *Ocean Science* 8, 845–857. <https://doi.org/10.5194/os-8-845-2012>

M. Kanamitsu, W. Ebisuzaki, J. Woollen, et al. 2002. NCEP–DOE AMIP-II Reanalysis (R-2). *Bull. Amer. Meteor. Soc.* 83, 1631–1644. <https://doi.org/10.1175/BAMS-83-11-1631>

R. A. Locarnini, A. V. Mishonov, O. K. Baranova, et al. 2018. *World Ocean Atlas 2018, Volume 1: Temperature*. A. Mishonov Technical Ed.

T. Naegler. 2009. Reconciliation of excess  $^{14}\text{C}$ -constrained global  $\text{CO}_2$  piston velocity estimates. *Tellus B: Chemical and Physical Meteorology* 61, 372–384. <https://doi.org/10.1111/j.1600-0889.2008.00408.x>

National Geophysical Data Center, 2006. 2-minute Gridded Global Relief Data (ETOPO2) v2. NOAA. <https://doi.org/doi:10.7289/V5J1012Q>

C. Rödenbeck, R. F. Keeling, D. C. E. Bakker, et al. 2013. Global surface-ocean  $\text{pCO}_2$  and sea–air  $\text{CO}_2$  flux variability from an observation-driven ocean mixed-layer scheme. *Ocean Sci.*, 9, 193–216. <https://doi:10.5194/os-9-193-2013>

R. Wanninkhof. 2014. Relationship between wind speed and gas exchange over the ocean revisited: Gas exchange and wind speed over the ocean. *Limnology and Oceanography: Methods* 12, 351–362. <https://doi.org/10.4319/lom.2014.12.351>

R. F. Weiss. 1974. Carbon dioxide in water and seawater: The solubility of a non-ideal gas. *Mar. Chem.* 2, 203–215.

## 4.5. ECOSSE

### 4.5.1. Model Description

The ECOSSE model was developed to simulate highly organic soils from concepts originally derived for mineral soils in the RothC (Jenkinson and Rayner, 1977; Jenkinson et al. 1987; Coleman and Jenkinson, 1996) and SUNDIAL (Bradbury et al. 1993; Smith et al. 1996) models. Following these established models, ECOSSE uses a pool type approach, describing soil organic matter (SOM) as pools of inert organic matter, humus, biomass, resistant plant material and decomposable plant material. All processes of the carbon and nitrogen dynamics are considered (Smith et al., 2010a,b). Additionally, in ECOSSE processes of minor relevance for mineral arable soils are implemented as well (e.g., methane emissions) to have a better representation of processes that are relevant for other soils (e.g., organic soils). ECOSSE can run in different modes and for different times steps. The two main modes are site specific and limited data. In the later version, basis assumptions/estimates for parameters can be provided by the model. This increases the uncertainty but makes ECOSSE a universal tool that can be applied for large scale simulations even if the data availability is limited. To increase the accuracy in the site-specific version of the model, detailed information about soil properties, plant input, nutrient application and management can be added as available.

Additional information can be found in the previous deliverables D3.4 and D3.5.

The previous version of ECOSSE provided results for heterotrophic respiration for daily time steps. To meet the needs of VERIFY, the ECOSSE model was extended to simulate NPP and yield through modification of internal routines. Based on the available NPP module (MIAMI model; Lieth,1972) we were able to simulate the annual NPP, which was allocated to aboveground and belowground biomass based on the study of Neumann and Smith (2018). This study also provided a generic harvest index to estimate the yield. This enabled simulation of the NBP for croplands. For grassland simulations, the allocation factors were adapted and the NPP simulations adapted for nutrient limitations. For the simulations reported here ECOSSE was run with a monthly time step, as this provided sufficient data for the target area and time steps.

#### 4.5.2. References/link

N. J. Bradbury, A. P. Whitmore, P. B. S. Hart, et al. (1993). Modelling the fate of nitrogen in crop and soil in the years following application of <sup>15</sup>N-labelled fertilizer to winter wheat. *J Agr Sci* 121: 363-379

K. Coleman, D. S. Jenkinson (1996). RothC-26.3 - A model the turnover of carbon in soil. In: Powlson DS, Smith P, Smith JU (ed) Evaluation of soil organic matter models using existing long-term datasets. NATO ASI Series I, vol. 38. Springer, Berlin, pp 237–246

D. S. Jenkinson, J. H. Rayner (1977). The turnover of organic matter in some of the Rothamsted classical experiments. *Soil Sci* 123: 298–305

D. S. Jenkinson, P. B. S. Hart, J. H. Rayner, et al. (1987). Modelling the turnover of organic matter in long-term experiments at Rothamsted. *INTECOL Bulletin* 15:1-8

H. Lieth (1972). Modelling the primary productivity of the earth. *Nature and resources, UNESCO, VIII*, 2:5-10.

J. U. Smith, N. J. Bradbury, T. M. Addiscott (1996). SUNDIAL: A PC-based system for simulating nitrogen dynamics in arable land. *Agron J* 88:38-43

J. U. Smith, P. Gottschalk, J. Bellarby, et al. (2010a). Estimating changes in national soil carbon stocks using ECOSSE – a new model that includes upland organic soils. Part I. Model description and uncertainty in national scale simulations of Scotland. *Climate Research* 45, 179-192. doi: 10.3354/cr00899.

J. U. Smith, P. Gottschalk, J. Bellarby, et al. (2010b). Estimating changes in national soil carbon stocks using ECOSSE – a new model that includes upland organic soils. Part II. Application in Scotland. *Climate Research* 45, 193-205. doi: 10.3354/cr00902.

J. Smith, P. Gottschalk, J. Bellarby, et al. (2011). Model to estimate carbon in organic soils—sequestration and emissions (ECOSSE) user-manual. University of Aberdeen, UK, pp 1–77

## 4.6. EFISCEN Space

### 4.6.1. Model Description

EFISCEN Space is a high-resolution model that describes the current structure and composition of forest resources at local to European scales. The model enables the assessment of the impact of forest management strategies, such as mobilisation strategies. EFISCEN Space simulates the forest as a collection of 1 ha model stands, where each model stand is representative of a larger area. Forest development for each model stand is modelled as the development of the number of trees per diameter class per tree species. There are 40 diameter classes of 2.5 cm width, starting with diameter class 1 at 0-2.5 cm. A maximum of 20 predetermined species groups can be used, corresponding to the most common tree species in Europe (Schelhaas et al., 2018a).

The model stands can be initialised using plot-based or stand-based forest inventory data from local to a national level. Transitions to a higher diameter class are derived from species-specific growth functions that are calibrated using a large set of observed diameter increment data across Europe (Schelhaas et al., 2018b). The growth functions are sensitive to diameter, basal area in the stand and a number of abiotic variables. The abiotic variables are derived from external databases where the locations of the model stands are used to extract specific information on abiotic and weather data.

Harvest and mortality are derived from observed local repeated NFI observations. Recruitment is not yet modelled. Diameters are converted to volume using local volume functions, usually derived from NFI data. The model runs on an annual timescale, with a minimum of one year. The model produces annual output on the forest state, mortality and harvest, expressed in terms of tree numbers, basal area and volume; per model stand, per species and per diameter class. These outputs are then converted to biomass values and subsequently to carbon. Outputs can be aggregated to yearly overviews per model stand or for the total modelled area. For use in the VERIFY project, outputs are aggregated (average per grid cell) according to the meteorological forcing grid provided within the project.

### 4.6.2. References/link

M. J. Schelhaas, J. Fridman, G. M. Hengeveld, et al. (2018a). Actual European forest management by region, tree species and owner based on 714,000 re-measured trees in national forest inventories. *PLoS ONE* 13(11), 23p.

M. J. Schelhaas, G. M. Hengeveld, N. Heidema, et al. (2018b). Species-specific, pan-European diameter increment models based on data of 2.3 million trees. *Forest Ecosystems* 5(21), 19p.

## 4.7. EPIC-IIASA

### 4.7.1. Model Description

The EPIC-IIASA model was integrated with VERIFY weather forcing CRUERA v 2.0 dataset covering the period 1981-2020, and a new version of atmospheric CO<sub>2</sub> concentration data was included. As in the previous deliverable D3.5, each cell of the 1-km simulation grid in EPIC-IIASA has been driven by the underlying daily meteorological inputs, including solar radiation, minimum and maximum temperature, precipitation, relative humidity, and wind speed. In this version, EPIC-IIASA was used to simulate cropland and grasslands with the following assumptions and input datasets:

#### Cropland:

- Land cover & terrain: CORINE2000 (arable land and heterogeneous agriculture area), where each 1-km grid cell was represented by a 50-ha field with a mode elevation and slope derived from the Shuttle Radar Topographic Mission Data (SRTM) digital elevation model (Werner, 2001).
- Soils: soil inputs derived from the European Soil Bureau Database (ESDB v2.0, <https://esdac.jrc.ec.europa.eu>), the map of organic carbon content in the topsoil (Lugato et al., 2014), and the Database of Hydraulic Properties of European Soils (Wösten et al., 1999).
- Crops: crop calendars of barley, corn maize, winter rapeseed, rice, winter rye, soybean, sunflower, winter wheat, sugar beet, and potatoes were adopted from Balkovič et al. (2018).
- Fertilization: crop specific nitrogen and phosphorus fertilizer application rates were adopted from Balkovič et al. (2018, 2013).
- Irrigation: crop specific irrigation was based on the European Irrigation Map (Wriedt et al., 2009).
- Crop residue handling: 20% of crop residues were harvested in case of cereals (excluding maize), while no residues were harvested for other crops (Köble, 2014).
- Soil cultivation: tillage consisting of two cultivation operations and moldboard ploughing prior to sowing, and an offset disking after harvesting of cereals, was implemented. Two row cultivations during the growing season were assumed for maize and one ridging operation for potatoes.

#### Grasslands:

- Land cover & terrain: CORINE2000 (permanent cropland, pastures, heterogeneous agricultural areas, shrub and herbaceous vegetation), elevation and slope derived from SRTM.
- Soils: same as for cropland, where a 20-year spin-up was used to initialize soil inputs.
- Three functional types of grasses with different optimum and base temperature requirements were used for the European simulations, namely winter pastures, brome grass, and fescue grass from the EPIC crop database.

- Grass type distribution mask: fescue grass type was used for the cooler and continental climate, while an average of fescue and winter pastures was used for the moderate and oceanic climate, and an average of brome and winter pastures was used for the Mediterranean climate.
- Annual carbon and nitrogen inputs (i.e., manure, fertilization, and atmospheric deposition) were introduced following the ISI-MIP3 modelling protocol.
- Two fHarvest intensities (low and moderate) were used to approximate the combined effect of grazing and mowing in Europe. The distribution of fHarvest across Europe was obtained by spatial aggregation of data from Chang et al (2016). Low intensity was approximated by one fHarvest operation with 50% harvest efficiency, while moderate intensity by two fHarvest operations with 80% harvest efficiency.

Daily simulations of the respective state variables and fluxes over the period 1981-2020 were aggregated with monthly resolution (annually for fHarvest). See Table 6 for the list of simulated outputs and the rules applied for temporal aggregation.

**Table 6 : EPIC-IIASA output variables.**

Variable	Unit	Description	Temporal aggregation
<b>mrso</b>	kg m <sup>-2</sup> month <sup>-1</sup>	Total Soil Moisture Content	1 <sup>st</sup> day of month
<b>mrro</b>	kg m <sup>-2</sup> month <sup>-1</sup>	Total Runoff, Drainage, and Subsurface Runoff	Monthly sum of daily fluxes
<b>evapotrans</b>	kg m <sup>-2</sup> month <sup>-1</sup>	Total Evapo-Transpiration	Monthly sum
<b>cVeg</b>	kg C m <sup>-2</sup> month <sup>-1</sup>	Carbon in Vegetation	1 <sup>st</sup> day of month
<b>clitter</b>	kg C m <sup>-2</sup> month <sup>-1</sup>	Carbon in Litter	Monthly sum
<b>cSoil</b>	kg C m <sup>-2</sup> month <sup>-1</sup>	Carbon in Soil	1 <sup>st</sup> day of month
<b>npp</b>	kg C m <sup>-2</sup> month <sup>-1</sup>	Net Primary Production - total	Monthly sum
<b>npp(a)</b>	kg C m <sup>-2</sup> month <sup>-1</sup>	Net Primary Production – aboveground	Monthly sum
<b>npp(b)</b>	kg C m <sup>-2</sup> month <sup>-1</sup>	Net Primary Production – belowground	Monthly sum
<b>rh</b>	kg C m <sup>-2</sup> month <sup>-1</sup>	Heterotrophic Respiration	Monthly sum
<b>fHarvest</b>	kg C m <sup>-2</sup> year <sup>-1</sup>	C Flux to Atmosphere from harvested crop biomass consumption	Last day of year
<b>yoc</b>	kg C m <sup>-2</sup> month <sup>-1</sup>	soil carbon loss with sediments (water erosion)	Monthly sum
<b>clch</b>	kg C m <sup>-2</sup> month <sup>-1</sup>	leached soluble carbon	Monthly sum
<b>nee</b>	kg C m <sup>-2</sup> month <sup>-1</sup>	Net ecosystem C exchange (grasslands only)	Monthly sum

### Aggregation of simulated outputs

The EPIC-IIASA simulation outputs were aggregated to represent carbon fluxes and stocks on managed cropland and grasslands. For cropland, first, crop-specific outputs were calculated in

each grid cell as a mean from rainfed and irrigated simulations, weighted by the area of irrigated and rainfed production based on the European Irrigation Map. Second, monthly variables from Table 6 were calculated in each grid cell as a mean value of the crop-specific output variables, weighted by harvested areas of crops reported by EUROSTAT. The harvested carbon (fHarvest) represents carbon exported with crop yield and harvested residues, again calculated as a weighted mean from the NUTS2-specific crop harvested areas. Finally, for conversion purposes, we assume that dry matter crop biomass contains 42% of carbon where applicable. For grasslands, monthly outputs simulated for all grass types were averaged based on the grass type distribution mask described above.

### Re-gridding

Simulation outputs (Table 6) were spatially re-gridded from a 1-km layout projected in ETRS\_1989\_LAEA coordinate system to a 0.125 x 0.125° CRUERA v 2.0 grid in the WGS84 coordination system. Mean values from all underlying EPIC-IIASA grid cells in a 0.125 x 0.125° cell were calculated. Output variables are organized according to the VERIFY simulation protocol.

### 4.7.2. References/link

J. Balkovič, R. Skalský, C. Folberth, et al. (2018). Impacts and Uncertainties of +2°C of Climate Change and Soil Degradation on European Crop Calorie Supply Earths Future 6 373–95

J. Balkovič, M. van der Velde, E. Schmid, et al (2013). Pan-European crop modelling with EPIC: Implementation, up-scaling and regional crop yield validation Agric. Syst. 120 61–75

J. Chang, P. Ciais, M. Herrero, et al. (2016). Combining livestock production information in a process-based vegetation model to reconstruct the history of grassland management Biogeosciences 13 3757–76

R. Köble. (2014) The Global Nitrous Oxide Calculator – GNOC – Online Tool Manual (European Union) Online:  
[http://gnoc.jrc.ec.europa.eu/documentation/The\\_Global\\_Nitrous\\_Oxide\\_Calculator\\_User\\_Manual\\_version\\_1\\_2\\_4.pdf](http://gnoc.jrc.ec.europa.eu/documentation/The_Global_Nitrous_Oxide_Calculator_User_Manual_version_1_2_4.pdf)

E. Lugato, P. Panagos, F. Bampa, et al. (2014). A new baseline of organic carbon stock in European agricultural soils using a modelling approach Glob. Change Biol. 20 313–26

M. Werner. (2001). Shuttle Radar Topography Mission (SRTM) Mission Overview Frequenz 55 75–9

J. R. Williams. (1995). The EPIC model, in: Singh, V.P. (Ed.), Computer models of watershed hydrology (Water resources publisher, Colorado) pp 909–1000

J. H. M. Wösten, A. Lilly, A. Nemes, et al. (1999). Development and use of a database of hydraulic properties of European soils *Geoderma* 90 169–85

G. Wriedt, M. van der Velde, A. Aloe, et al. (2009). A European irrigation map for spatially distributed agricultural modelling *Agric. Water Manag.* 96 771–89

## 4.8. Fluxcom

### 4.8.1. Model Description

This model was referred to as “Statistical upscaling of eddy covariance fluxes” in previous deliverables, and is changed here for consistency with the literature.

Fluxcom2.0 is the successor of the data-driven modelling approach Fluxcom. As with the original Fluxcom, in Fluxcom2.0 terrestrial carbon fluxes from eddy-covariance measurements, meteorological observations and Earth observation data are combined with machine-learning models to produce spatially continuous carbon flux estimates using gridded products of the same predictor variables. For a detailed description of Fluxcom please refer to reports D3.4 and D3.5.

For this reporting year, we produce three-hourly estimates of NEE for Europe at a spatial resolution of 0.05deg for the years 2002-2020. The following predictor variables are used for this deliverable:

- Air temperature
- Specific humidity
- Wind speed
- Longwave incoming radiation
- Shortwave incoming radiation, potential and actual
- Derivative of potential shortwave incoming radiation
- EVI and information on its gapfilltype
- kNDVI and information on its gapfilltype
- NDWI and information on its gapfilltype
- Land surface temperature, MODIS TERRAday, TERRAnight, AQUAday, AQUAnight and information on their respective gapfilltype
- ‘Fuzzy’ categories of vegetation types: trees, shrubs, grasses, evergreen, deciduous, broadleaf, needleleaf, water, wetland, unvegetated, C4, managed

In the new set-up, major efforts have been invested into harmonizing site-level training data from recently-available eddy covariance dataset releases LaThuile, Fluxnet 2015 (Pastorello et al. 2020) and the ICOS drought 2018 initiative (ICOS drought) and into their quality screening and gapfilling for some of their variables. In addition, MODIS satellite observations of surface reflectance and land surface temperature have been updated to the most recent version. Their preprocessing in terms of quality checks, gapfilling and the set of indices computed from the

reflectances have been improved. Cutouts of several pixels around a given tower from the MCD43A4 and MCD43A2 datasets for the reflectances, and from the MOD11A1 and MYD11A1 datasets for land surface temperature are used for the training. The number of pixels or their distance to the tower is not fixed for a given site but selected based on data availability within a maximum distance of 2km around a tower. For the production of spatially explicit flux estimates, the MODIS MCD43C4, MOD11C1 and MYD11C1 daily products in 0.05deg spatial pixels were used. According to the common modelling protocol within VERIFY WP3, meteorological datasets from CRUHAR/CRUERA as well as land cover information from the HILDA+ dataset are used as predictor datasets in the forward runs. The meteorological fields are bilinearly interpolated from their native 0.125deg resolution to 0.05deg. Land cover classes are aggregated from 1km to 0.05deg by the dominant cover in a given 0.05deg pixel. The creation of fuzzy classes of vegetation types allowed for different plant functional type classification schemes, i.e., IGBP which is reported for in situ data and Hilda+ for global land cover, to be used as a common predictor. Boosted regression trees (Chen and Guestrin 2016) were used as the machine learning method.

#### **4.8.2. References/link**

G. Pastorello, C. Trotta, E. Canfora, et al. (2020). The FLUXNET2015 dataset and the ONEFlux processing pipeline for eddy covariance data. *Sci Data* 7, 225. <https://doi.org/10.1038/s41597-020-0534-3>

Drought 2018 Team and ICOS Ecosystem Thematic Centre (2020). Drought-2018 ecosystem eddy covariance flux product for 52 stations in FLUXNET-Archive format, doi:[10.18160/YVR0-4898](https://doi.org/10.18160/YVR0-4898)

T. Chen and C. Guestrin. (2016). Xgboost: A scalable tree boosting system. *Proceedings of the 22nd acm sigkdd international conference on knowledge discovery and data mining*, pp. 785-794. <https://doi.org/10.1145/2939672.2939785>

### **4.9. G4M+FLAM**

#### **4.9.1. Model Description**

IIASA's G4M and FLAM models were linked to IIASA-EPIC via similar infrastructure based on simulation units. The geographical grid of regular grid cells with a spatial resolution of 5 x 5 arc min (about 8 km at the equator) covers geographical Europe. The resolution was increased compared to simulations for the previous year of the VERIFY project. Each grid cell used soil information preprocessed by the IIASA-EPIC group from the Harmonized World Soil Database. In particular, the available water capacity (AWC) parameter is used by G4M for the water balance calculations to take into account water stress on forest growth. The common simulation

infrastructure also includes various landscape parameters (e.g., elevation and slope) used in the modeling.

For model calibration and validation, we used aboveground biomass (AGB) maps from the GlobBiomass project, burned areas from the MODIS CCI dataset, and MODIS NPP.

For the climate inputs we use the aligned CRUERA dataset provided by the VERIFY project (1981-2020). The data on meteorological inputs including solar radiation, minimum and maximum temperature, precipitation, relative humidity, and wind speed is used for simulations covering 2010-2020. The data is preprocessed to fit the spatial resolution of 5 x 5 arc min. In addition, we used land-cover maps provided by the VERIFY project, i.e., the Hilda+ dataset.

See Table 7. for the list of simulated outputs.

**Table 7 : G4M/FLAM output variables of the carbon cycle. Output variables are organized according to the VERIFY simulation protocol.**

Variable	Unit	Description	Temporal aggregation
<b>FCO2_NPP_FOR</b>	kg C m <sup>-2</sup> yr <sup>-1</sup>	FCO2_NPP_FOR / Fluxes per square meter of forest	Annual
<b>AGB</b>	kg C m <sup>-2</sup>	Above Ground Biomass	Annual

### Re-gridding

Simulation outputs from Table 7 were spatially re-gridded to the 0.125 x 0.125° CRUERA V2.0 grid in the WGS84 coordination system.

### 4.9.2. References/link

G. Kindermann, S. Schoerghuber, T. Linkosalo, et al. (2013). Potential stocks and increments of woody biomass in the European Union under different management and climate scenarios. Carbon Balance and Management 8 (1) DOI:10.1186/1750-0680-8-2.

N. Khabarov, A. A. Krasovskii, M. Obersteiner, et al. (2016). Forest fires and adaptation options in Europe. Regional Environmental Change 16 (1): 21-30. DOI:10.1007/s10113-014-0621-0.

FAO, IIASA. Harmonized World Soil Database (Version 1.2). (FAO; IIASA, 2012).

M. Santoro. (2018). GlobBiomass - global datasets of forest biomass. doi:10.1594/PANGAEA.894711

M. Santoro and O. Cartus (2019). ESA Biomass Climate Change Initiative (Biomass\_cci): Global datasets of forest above-ground biomass for the year 2017, v1.

doi:10.5285/BEDC59F37C9545C981A839EB552E4084

<https://catalogue.ceda.ac.uk/uuid/bedc59f37c9545c981a839eb552e4084>

M. L. Pettinari, J. Lizundia-Loiola, E. Chuvieco. (2020). ESA CCI ECV Fire Disturbance: D4.2 Product User Guide-MODIS, version 1.0. Available at: <https://www.esa-fire-cci.org/documents>

S. W. Running, R. R. Nemani, F. A. Heinsch, et al. (2004). A continuous satellite-derived measure of global terrestrial primary production *BioScience* **54** 547–60

K. Winkler, R. Fuchs, M. D. A. Rounsevell, et al. (2021). Global land use changes are four times greater than previously estimated. *Nature Communications*, 12(2501), <https://doi.org/10.1038/s41467-021-22702-2>

## 4.10. Lateral fluxes

### 4.10.1. Model Description

For the lateral fluxes, we used an effort conducted in the European project CoCO<sub>2</sub> in which high-resolution maps of annual sources and sinks of CO<sub>2</sub> from wood trade, crop trade, and rivers have been calculated for each year at fairly high global spatial resolution between the years 1961 and 2019. The focus of the work was carbon transport at long distances (> 50 km). For trade fluxes, statistics from the Food and Agriculture Organization of the United Nations (FAO) have been analyzed with appropriate conversion factors and disaggregated on a 0.08-degree global grid with a series of proxies and activity maps. River fluxes come from a data-driven climatology. For croplands, the populations of people and animals are used as proxies to identify where the carbon may be emitted. For wood products, a bookkeeping model was built to account for the storage pools in construction and landfills.

A first version was delivered in August 2021. A second version delivered in December 2021 extended the maps to the year 2020. One major change for all years was the explicit inclusion of biofuel sinks and sources from crop and wood, in collaboration with Yilong Wang (*Institute of Geographical Sciences and Natural Resources Research, China*). To that end, trade statistics from the International Energy Agency (IEA) and spatial distribution maps from Peking University (PKU) have been included in the processing.

In VERIFY, we have processed the global maps to derive country- and regional-level lateral fluxes in the European Union.

### 4.10.2. References/link

P. Ciais, P. Bousquet, A. Freibauer, et al. (2007). Horizontal displacement of carbon associated with agriculture and its impacts on atmospheric CO<sub>2</sub>, *Global Biogeochem. Cycles*, 21, GB2014, doi:[10.1029/2006GB002741](https://doi.org/10.1029/2006GB002741).

P. Ciais, A. Bastos, F. Chevallier, et al. (2020). Definitions and methods to estimate regional land carbon fluxes for the second phase of the REgional Carbon Cycle Assessment and Processes Project (RECCAP-2), *Geosci. Model Dev. Discuss.* [preprint], <https://doi.org/10.5194/gmd-2020-259>, in review.

P. Ciais, Y. Yao, T. Gasser, et al. (2021). Empirical estimates of regional carbon budgets imply reduced global soil heterotrophic respiration, *National Science Review*, Volume 8, Issue 2, February 2021, nwa145, <https://doi.org/10.1093/nsr/nwa145>

## 4.11. ORCHIDEE

### 4.11.1. Model Description

ORCHIDEE is the land surface model of the IPSL (Institut Pierre Simon Laplace) Earth System Model. Hence, by conception, the ORCHIDEE model can be run coupled to a global circulation model. In this deliverable, as in previous deliverables, ORCHIDEE was run offline as a stand-alone land surface model. The stand-alone configuration receives the atmospheric conditions such as temperature, humidity and wind, to mention a few, from so-called “forcing files”. Unlike the coupled set-up, which needs to run at the global scale (but with the possibility of a regional zoom), the stand-alone configuration can cover any area ranging from the global domain to a single grid point.

As in previous years, version 2.2 of ORCHIDEE (ORC2.2) was used to calculate carbon fluxes from forests, grasslands, and croplands across Europe using the CRUHAR/CRUERA forcing data provided by the project from 1901-2020. The reader is referred to D3.4 and D3.5 for more details about ORC2.2. In addition, a version of ORCHIDEE which includes dynamic nitrogen cycling (Vuichard et al, 2019) was run in VERIFY for the first time. This version of the model, referred to alternatively as ORC3 or ORCHIDEE-N, explicitly accounts for the impact of nitrogen limitation in the leaf on photosynthesis and includes various reactions in the soil which converts nitrogen into different forms and affects uptake by plants. This required the use of additional datasets not considered last year, for which we were able to use nitrogen deposition data supplied through the VERIFY project (see deliverable D3.3).

### 4.11.2. References/link

N. Vuichard, P. Messina, S. Luyssaert, et al. (2019). Accounting for carbon and nitrogen interactions in the global terrestrial ecosystem model ORCHIDEE (trunk version, rev 4999): multi-scale evaluation of gross primary production. *Geoscientific Model Development*, European Geosciences Union, 12 (11), pp.4751-4779.

## 5. Model Results

### 5.1. BLUE

Replacing LUH2, which is the land-use change forcing used in the Global Carbon Project's annual global carbon budget, in BLUE with the newest HILDA+ dataset at the same resolution results in significant temporal differences of LULCC emission estimates. While the total LULCC emission estimates based on HILDA+ and LUH2 are comparable in size and trends for overall Europe since 1960, single component fluxes differ substantially (Figure 3).

Accordingly, emissions from cropland expansion remain stable around  $80 \text{ TgC*yr}^{-1}$  based on HILDA+, whereas based on LUH2 crop emissions decrease until 2003 to then increase massively thereafter. Between 1960 and 2019, the difference in mean crop emissions between LUH2- and HILDA+-based simulations is  $40.0 \text{ TgC*yr}^{-1}$ . In comparison, the difference in mean ELUC is “only”  $4.5 \text{ TgC*yr}^{-1}$  in the same time period.

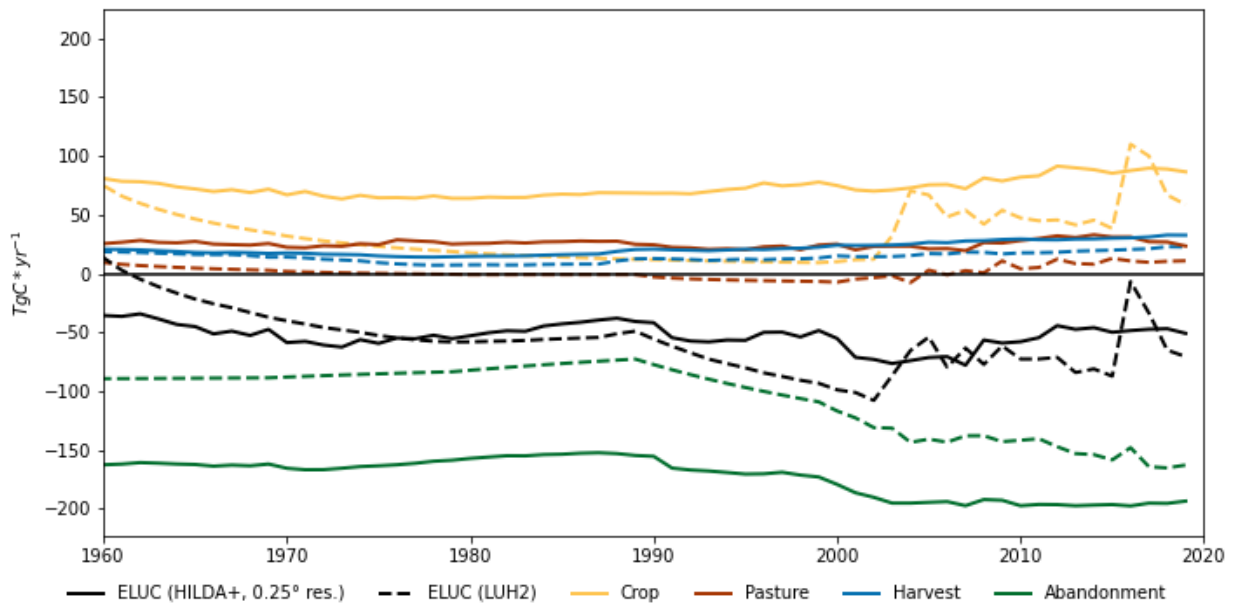


**Figure 3 : Estimates of ELUC and component fluxes based on HILDA+ (0.25°res.) and LUH2**

Similar to the crop emissions, emissions from pasture expansion are higher in runs with HILDA+ compared to runs with LUH2 (difference of mean:  $24.0 \text{ TgC*yr}^{-1}$ ). The most plausible reason for this difference is a different definition of “pasture areas”, as more areas are classified as pasture in HILDA+.

While the trends of carbon uptake following abandonment of cropland and pasture areas are similar between runs using HILDA+ and LUH2, the magnitude of the carbon sink differs (difference of mean:  $66.9 \text{ TgC*yr}^{-1}$ ). The larger sink in the HILDA+-based simulations partly

compensates the larger source from cropland and pasture, resulting in similar overall ELUC estimates.

Harvest estimates are very similar, which is less surprising given the fact that they are both based on LUH2. However, smaller differences exist due to the reallocation described above (mean difference  $7.4 \text{ TgC*yr}^{-1}$ ).

Extreme values in ELUC estimates based on LUH2 (i.e., 2004, 2015), which were most likely artifacts, are not present in the estimates based on HILDA+. This suggests a higher reliability of estimates based on HILDA+.

For the time period 1960-2019, the difference in mean ELUC for BLUE runs based on HILDA+ at  $0.01^\circ$  and  $0.25^\circ$  resolution is quite small ( $5.3 \text{ TgC*yr}^{-1}$ ). However, results show remarkable differences in the estimates of component fluxes. Similar to the estimates with different LULCC forcings, emissions from cropland and pasture expansion are higher (difference of mean:  $30.2 \text{ TgC*yr}^{-1}$ ,  $14.2 \text{ TgC*yr}^{-1}$ ) and the carbon uptake from abandonment is larger (difference of mean:  $-55.6 \text{ TgC*yr}^{-1}$ ) in the simulations at  $0.25^\circ$  resolution.

## 5.2. CABLE-POP

Figure 4 shows the decadal mean of the net biome productivity (NBP) across the simulation domain of Europe for 2010-2019 from the S3 simulation of the CABLE-POP model. There is some “graininess” present in the model because monthly and annual results are still very grainy in some areas, presumably due to the imprint of the LUH2 forcing at  $0.25\text{deg}$  which seems to have significant effects on the NBP in S3.

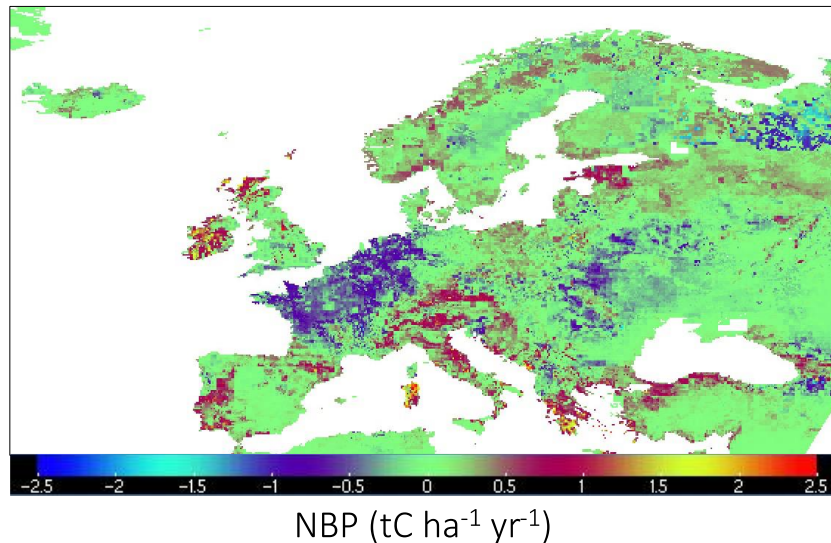


**Figure 4 : The net biome productivity from the CABLE-POP S3 run for 2010-2019.**

### 5.3. CBM-CFS3

Updated results from CBM show that the forest NBP for the period 2000-2015 for EU-25 + UK is on average 0.78 Mg C ha<sup>-1</sup> year<sup>-1</sup>, ranging from around 0.20 Mg C ha<sup>-1</sup> year<sup>-1</sup> for Hungary to about 1.54 Mg C ha<sup>-1</sup> year<sup>-1</sup> for the UK (see Figure 5). Based on our simulations, the NBP for EU25 + UK decreases by about 13% (highest drop in Sweden) when passing from the historical period (2000-2015) to 2020 (see Figure 6). The NBP is calculated based on a total forest area of about 158 million ha.

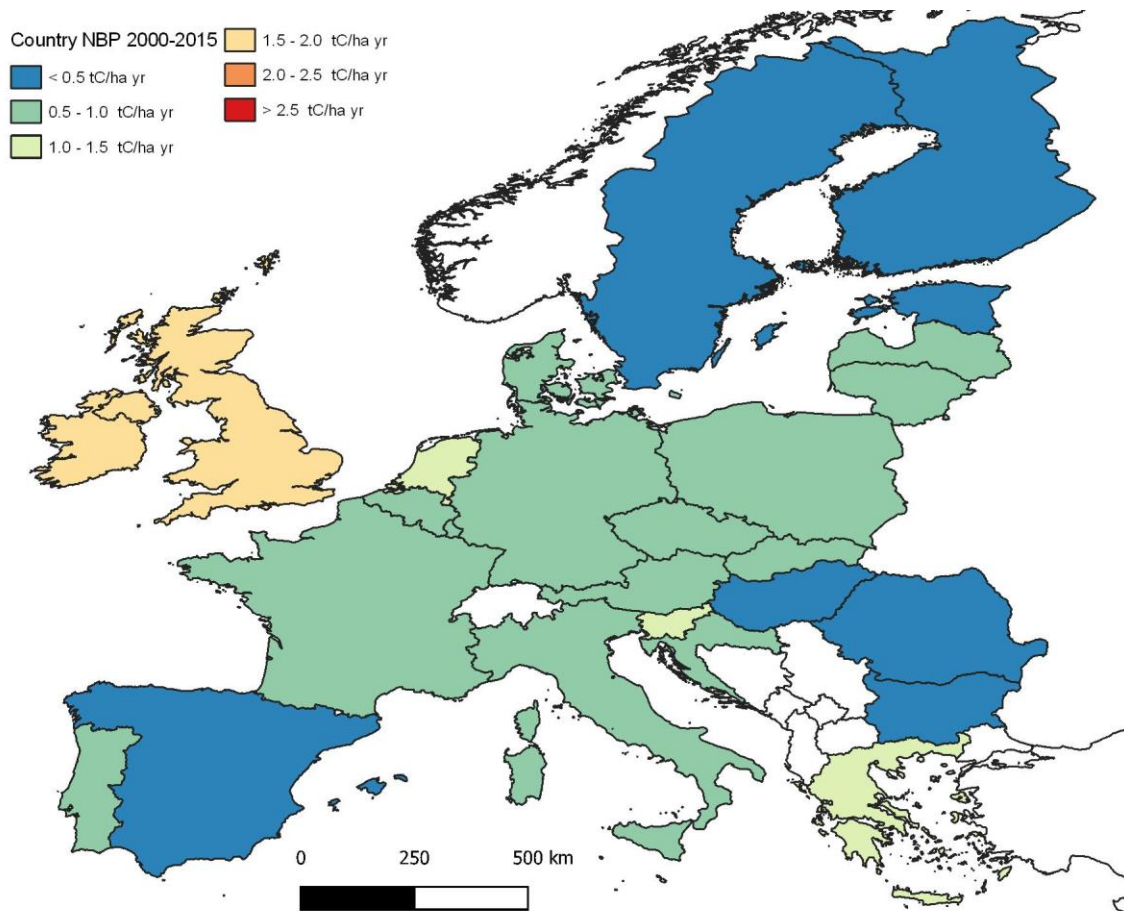


**Figure 5 : distribution of NBP (Mg C ha<sup>-1</sup> year<sup>-1</sup>) for EU-25 + UK for the period 2000-2015 (NUTS-0 level).**

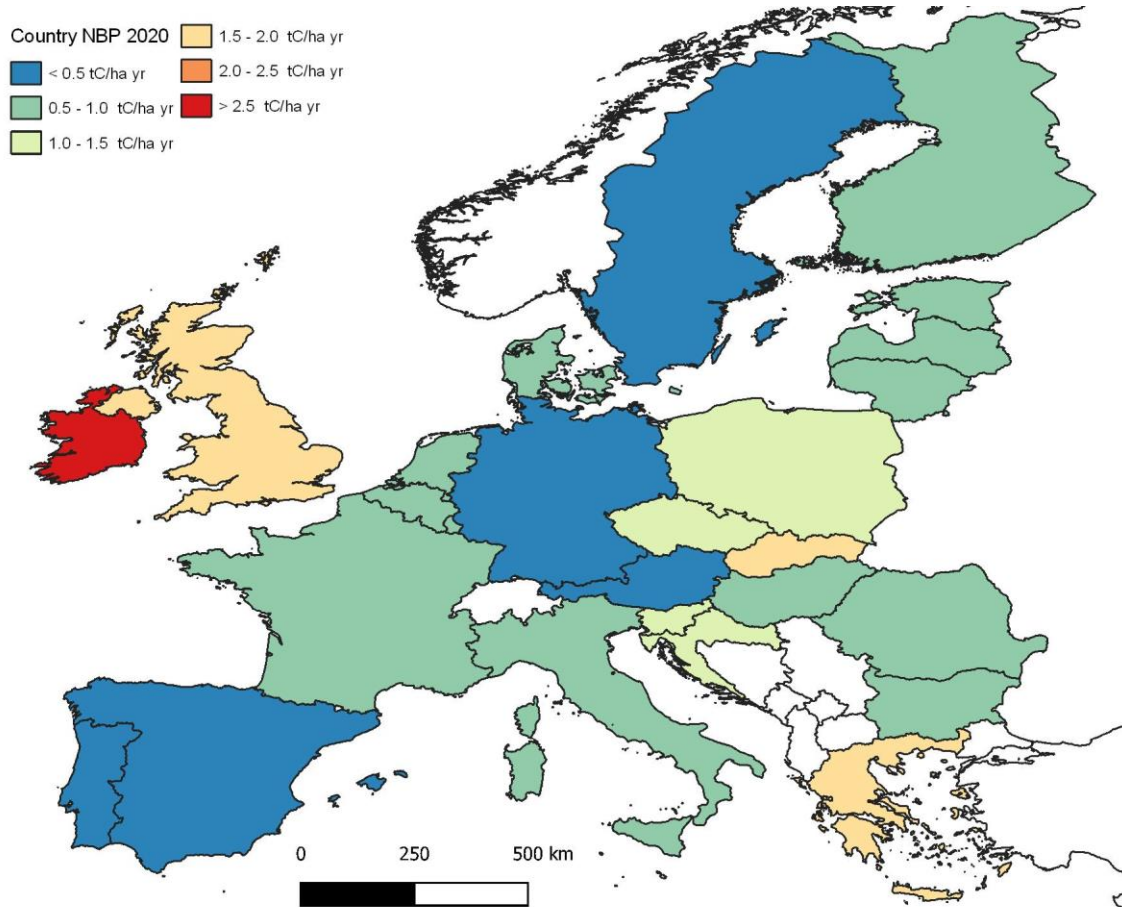


**Figure 6 : distribution of NBP (Mg C ha<sup>-1</sup> year<sup>-1</sup>) for EU-25 + UK for the year 2020 (NUTS-0 level), based on the continuation of historical management practices, as defined within the period 2000 - 2015.**

According to Pilli et al. (2017), the NBP corresponds to 16% of the NPP in managed forest land for the period 2000-2012. Uncertainties are only available for NPP. The overall uncertainty related to the living biomass stock is about 6.6% (based on simulations in Pilli et al. 2017). If compared to other models, the NPP from CBM is -17% than from EFISCEN, -8% than from BIOME-BGC, -16% than from ORCHIDEE, and +24% than from JULES (see Pilli et al. 2017). It should be noted that the versions of ORCHIDEE and EFISCEN used in Pilli et al. 2017 are not necessarily identical to the versions used in this deliverable.

### 5.3.1. References/link

R. Pilli, G. Grassi, W. A. Kurz, et al. (2017). The European forest sector: past and future carbon budget and fluxes under different management scenarios, *Biogeosciences*, 14, 2387–2405, <https://doi.org/10.5194/bg-14-2387-2017>.

## 5.4. Coastal ocean fluxes

The coastal fluxes were merged with daily open ocean fluxes from the Jena CarboScope ocean flux product version oc\_v2021 (Rödenbeck et al, 2013). In the merged version, the coastal product was selected for the regions in which it exists, and the open ocean product was used in all other regions.

The version used in this deliverable is v2021.2. Results for the merged product are shown in Figure 7.

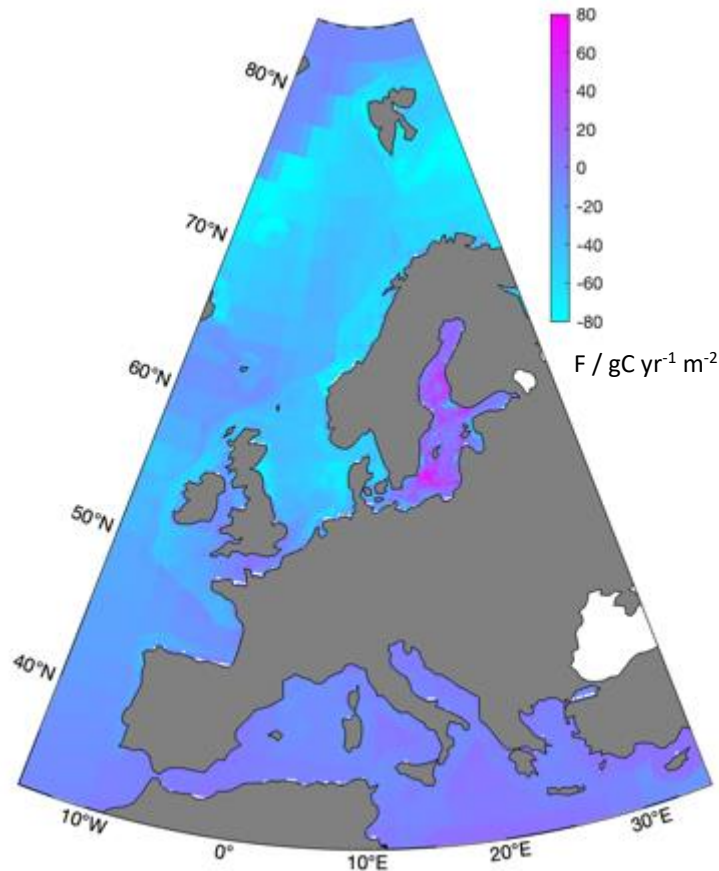


Figure 7 : Average air-sea flux in 2020.

## 5.5. ECOSSE

Former results for croplands were given as simulated emissions without considering the actual applied amounts of fertilizer, without crop specific separation of the results, in monthly time steps, and in a relatively coarse resolution of 0.25 degrees (deliverable D3.5). The latest (still preliminary) results addressing these limitations show an improvement. A reduction of the timestep from monthly to daily has improved the accuracy. Challenges were faced in the implementation of other changes, including the requirement of additional datasets not included

in D3.3, such as other sources of applied amounts of fertilizer and phenological data linked to agricultural management. In addition, the move towards a higher resolution required spin-up runs, lengthening the simulation times considerably. Therefore, we present here only preliminary results for croplands in a coarser (still 0.25 degree) resolution for the target period 1981-2020. In order to improve grassland results, structural changes are needed in the model which have not yet been finished.

In comparison to previous deliverables the results show a significantly reduced carbon sink (a European-wide sink of about  $4 \text{ g C m}^{-2}$  for the 40-year average), which is more in line with the inventories, other simulation results (e.g., EPIC and ORCHIDEE) and with literature (e.g., Ciais et al., 2010). The time series (Figure 8) shows fluctuation around zero for the NBP with a trend towards a small sink.

The analysis of absolute values is still ongoing, using the HILDA land use data provided in the VERIFY project (Figure 9). Preliminary results show an overall source of  $9.9 \text{ Tg C yr}^{-1}$ , which is very different than previous results and closer to the European inventories which show a source of  $5.6 \text{ Tg C yr}^{-1}$ . Further analysis will include examination of the discrepancies between ECOSSE results and the inventories (e.g., different land use data).

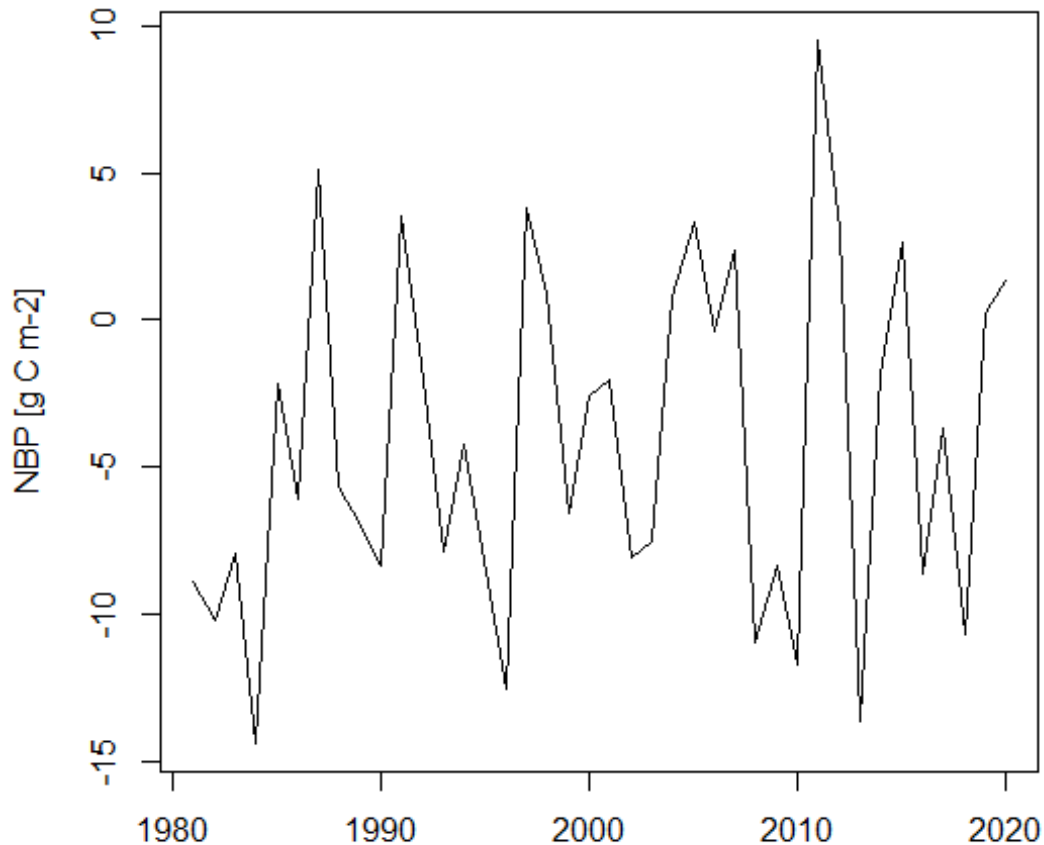


**Figure 8 : Annual spatial averages of the European NBP for 1981-2020 for croplands (only wheat is considered).**

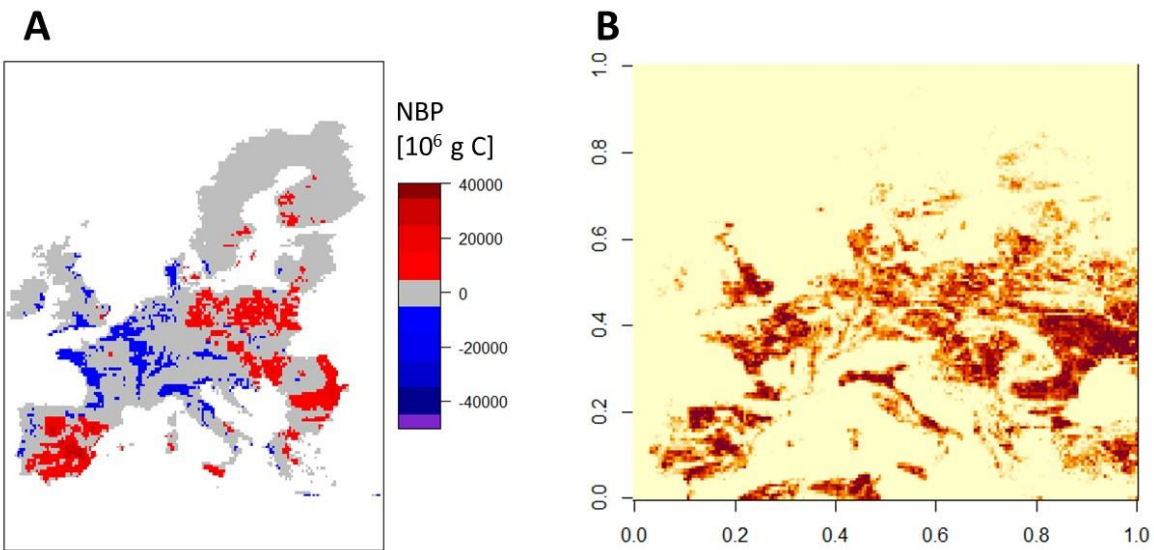


**Figure 9 : NBP as absolute values per pixel (A) and the distribution of cropland area (in km<sup>2</sup>) as the 40-year average of the HILDA land use/land cover data (B).**

P. Ciais, M. Wattenbach, N. Vuichard, et al. (2010). The European carbon balance. Part 2: croplands. *Global Change Biology*, 16: 1409-1428. <https://doi.org/10.1111/j.1365-2486.2009.02055.x>

## 5.6. EFISCEN Space

In 2020, the net biome productivity in the forests of fifteen European countries was modelled. The development of growing stock, increment and harvest volumes was also modelled. For each country an individual country report was written, with main findings from the simulations. The country reports were sent out to the contact persons of each country including country-specific questions. Almost all contact persons provided feedback to the country reports. This enabled refinement of the simulations, e.g., replacing generic harvest patterns and volume functions with country-specific patterns and functions. shows results for Germany for the harvest rate, increment, and growing stock.

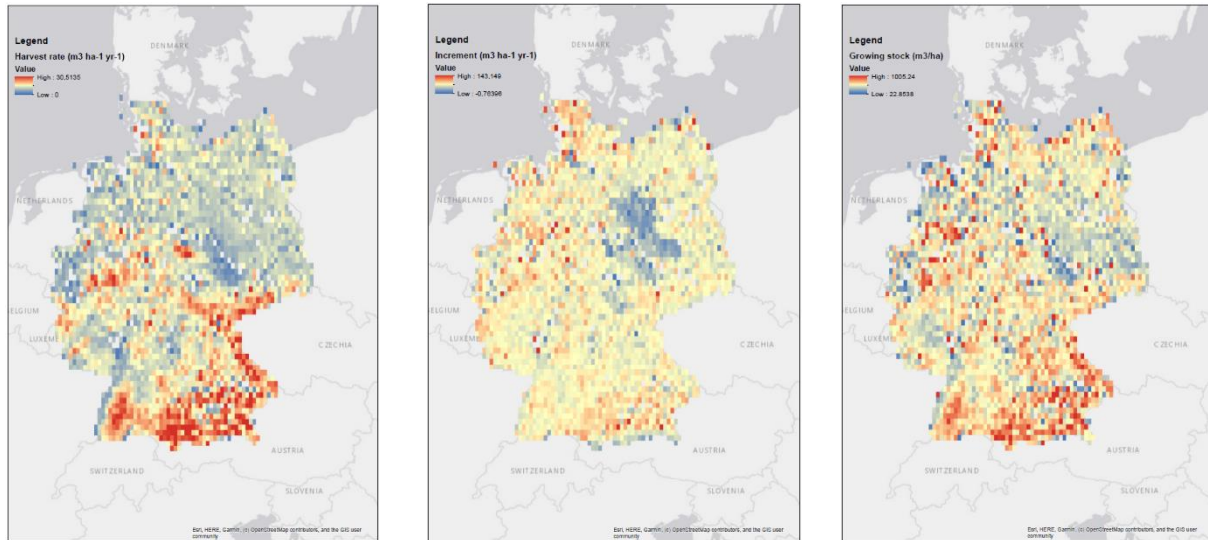


**Figure 10 : Modelled harvest rate, increment and growing stock for Germany**

New simulations for the countries will include soil carbon using the Yasso module (Järvenpää et al. 2015, Järvenpää et al. In prep.). Figure 11 shows the soil carbon stock and soil carbon flux in Germany. The average value for soil carbon stock was 215.0 tonnes C ha<sup>-1</sup>. The average value for soil carbon flux was 250.0 kg C ha<sup>-1</sup> yr<sup>-1</sup>. Figure 12 shows the distribution of the soil carbon stocks and fluxes across Germany based on pixel-level data.

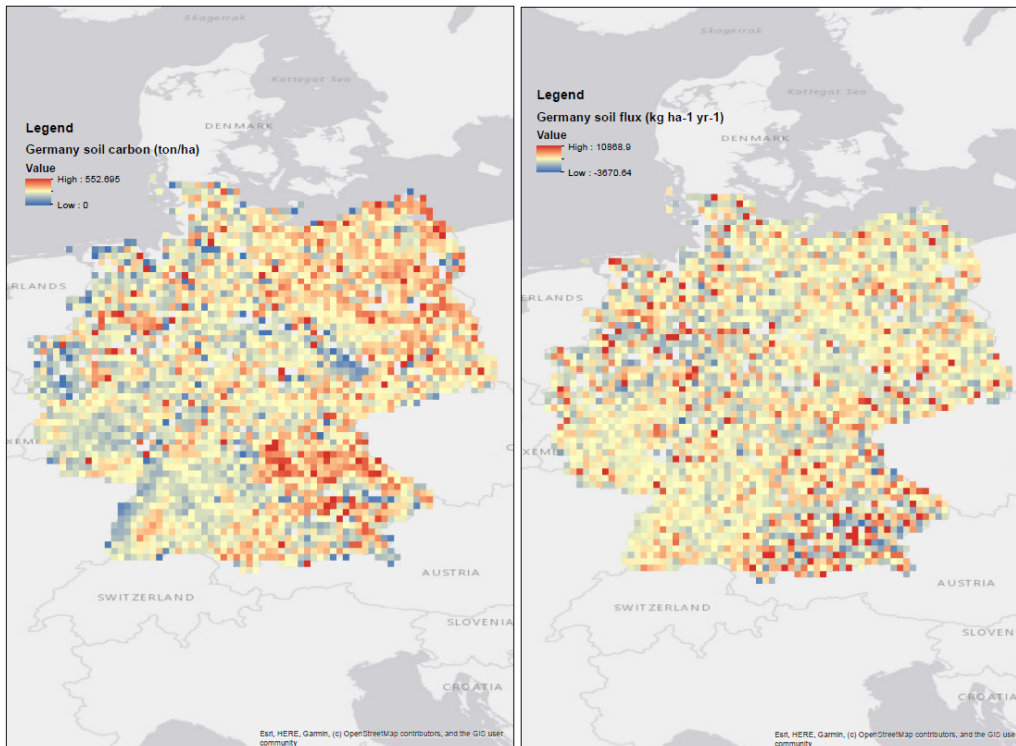


**Figure 11 : Maps of soil carbon stock (ton C ha<sup>-1</sup>) and soil carbon flux (kg C ha<sup>-1</sup> yr<sup>-1</sup>) (negative values are emissions)**

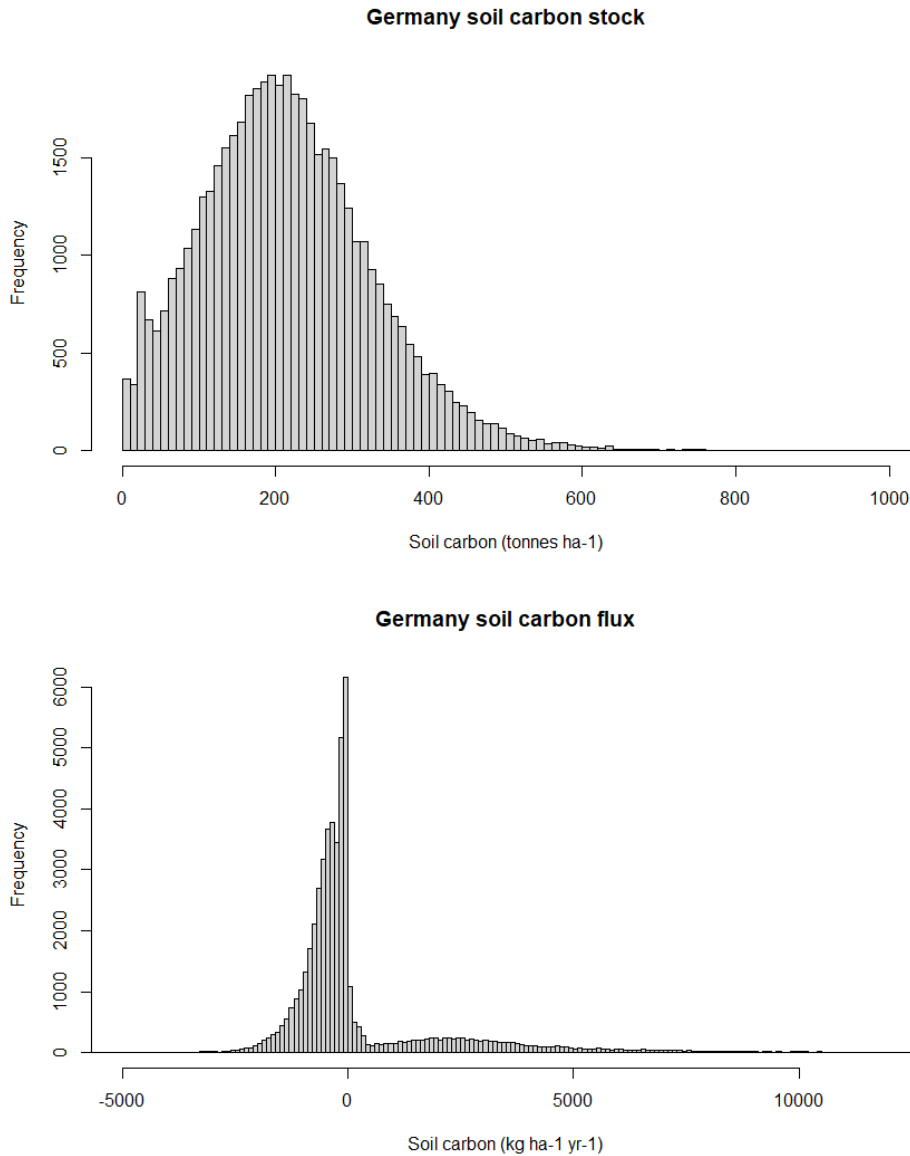


**Figure 12 : Histograms of soil carbon stock (ton C ha<sup>-1</sup>) and soil carbon flux (kg C ha<sup>-1</sup> yr<sup>-1</sup>) (negative values are emissions)**

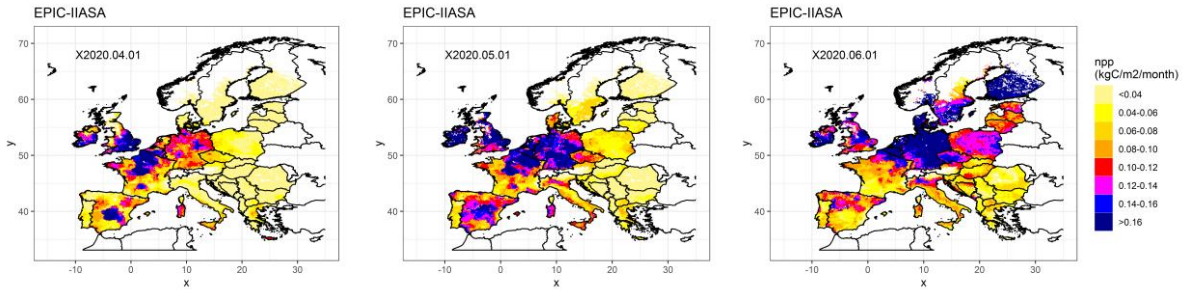
M. Järvenpää, A. Repo, A. Akujärvi, et al. (in prep). Soil carbon model Yasso 15: Bayesian calibration using worldwide litter decomposition and carbon stock data.

M. Järvenpää, A. Repo, A., Akujärvi, et al. (2015). Bayesian calibration of Yasso15 soil carbon model using global-scale litter decomposition and carbon stock measurements. Oral presentation at the 5th Nordic–Baltic Biometric Conference, Reykjavik, June 8–10 2015. Retrieved from <http://math.tut.fi/inversegroup/material/jarvenpaa2015bayesian.pdf>

### 5.7. EPIC-IIASA

We present below example results from re-gridded simulations for the year 2020 as driven by the CRUERA v2.0 meteorological forcing: NPP (npp, in  $\text{kg C m}^{-2} \text{ month}^{-1}$ ) and heterotrophic respiration (rh, in  $\text{kg C m}^{-2} \text{ month}^{-1}$ ) in Figures 13 and 14, respectively, for both cropland and grasslands.

(a)



(b)

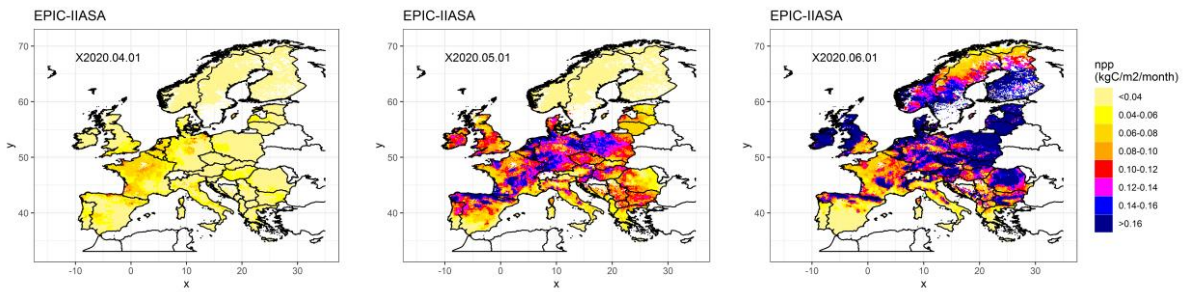


**Figure 13 : Mean NPP ( $\text{kg C m}^{-2} \text{ month}^{-1}$ , April to Jun 2020) on (a) cropland, and (b) grasslands calculated by EPIC-IIASA (CRUERA v 2.0).**

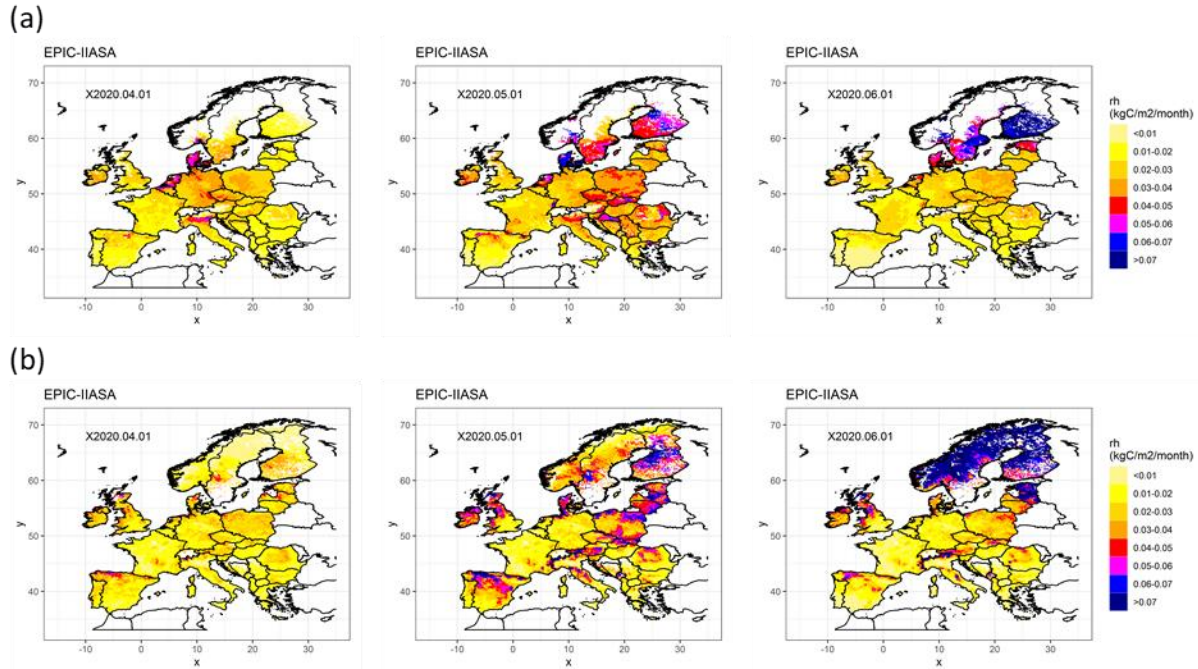


**Figure 14 : Mean rh (in kg C m<sup>-2</sup> month<sup>-1</sup>, April to Jun 2020) on (a) cropland, and (b) grasslands calculated by EPIC-IIASA (CRUERA v 2.0).**

### 5.8. Fluxcom

Figures 15 and 16 illustrate average spatial and temporal patterns of simulated NEE across Europe as obtained from Fluxcom2.0.

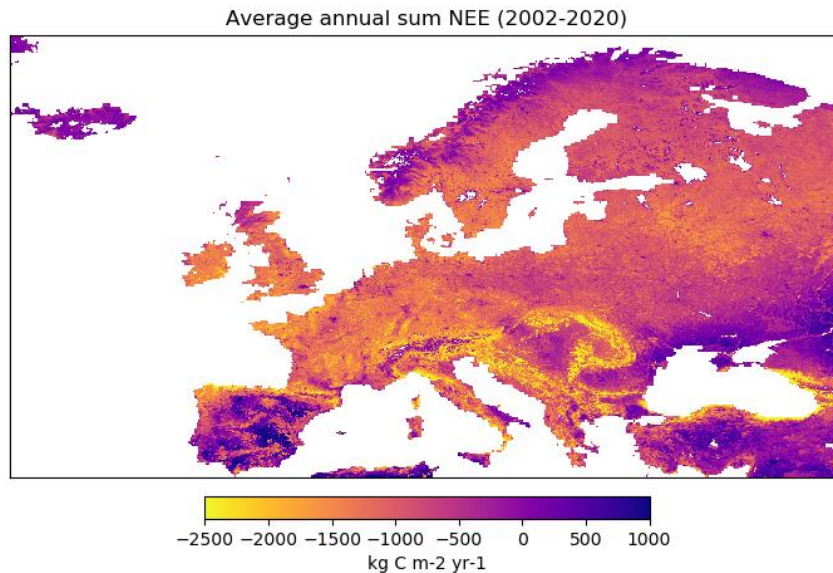


**Figure 15 : Average annual NEE simulated over the period 2002-2020, summed from 3-hourly NEE estimates per year.**

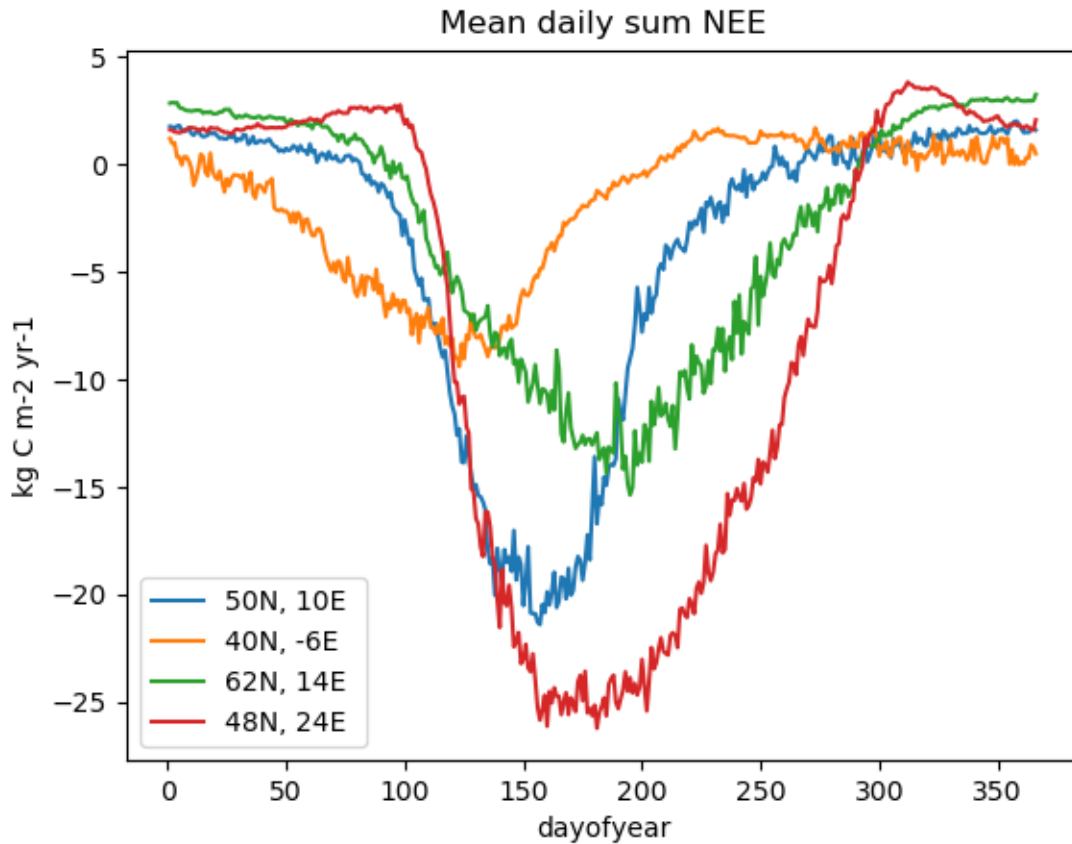


**Figure 16 : Average per day of year (2002-2020) of daily sums of simulated NEE at four different locations in Europe.**

Comparing to independent NEE estimates we find that the estimated sink strength is very strong, and even more unrealistic than previous data-driven estimates from Fluxcom v1. Investigating this issue, we found that shortwave incoming radiation in the CRUHAR/CRUERA meteorological datasets is on average 15% higher than both site-level measurements (Figure 17) and ERA5 values at the tower locations, with a seasonal trajectory of the bias and largest differences during summer time. Other meteorological variables, like air temperature, have a much more linear relationship between site-level and CRUHAR/CRUERA. We therefore did an experiment in predicting the European flux with CRUHAR/CRUERA SW\_IN reduced by 15%. This resulted in a reduction of the estimated NEE by an average of 21% (Figure 18). We also found that an additional but comparatively much smaller part of the differences can be explained by differences in temporal resolution between the training data (hourly) and the predictions (3-hourly).

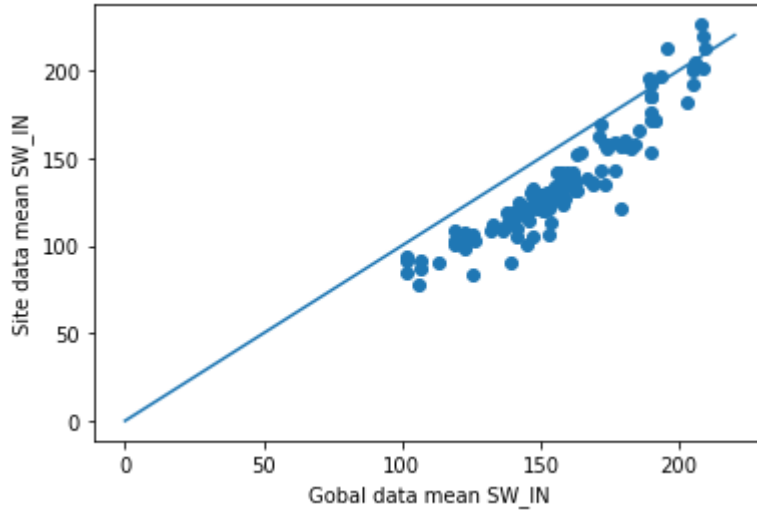


**Figure 17 : Comparison of shortwave incoming radiation at sites in Europe (each dot represents a site). Shown are the long term means for the CRUHAR/CRUERA extracted at the site coordinates versus the in-situ measured incoming shortwave radiation**

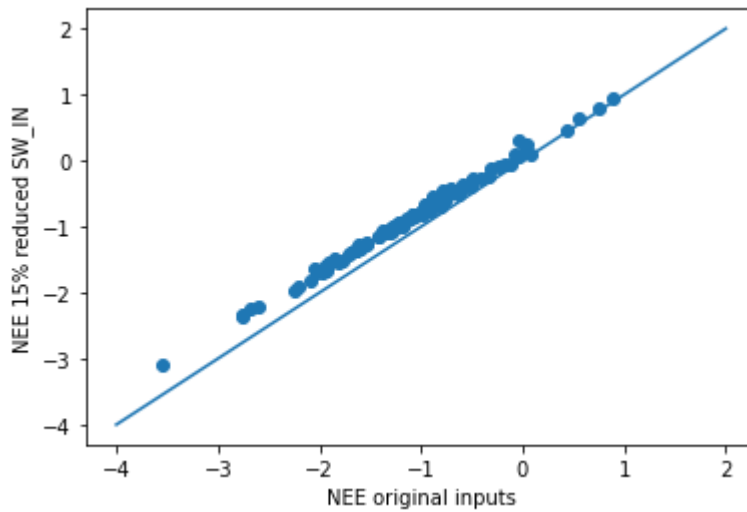


**Figure 18 : Comparison of predicted NEE with the original CRUHAR/CRUERA SW\_IN and the experiment in which NEE was predicted using CRUHAR/CRUERA SW\_IN reduced by 15%. Shown is average predicted NEE in the pixels containing European towers**

### 5.9. G4M+FLAM

We present some example results from re-gridded simulations for the year 2020 as driven by the CRUERA v2.0 meteorological forcing provided in the VERIFY project: NPP (the variable FCO2\_NPP\_FOR, in units of  $\text{kg C m}^{-2} \text{ month}^{-1}$ ) and aboveground biomass (AGB,  $\text{kg C m}^{-2}$ ) for forests across Europe in Figures 19 and 20.

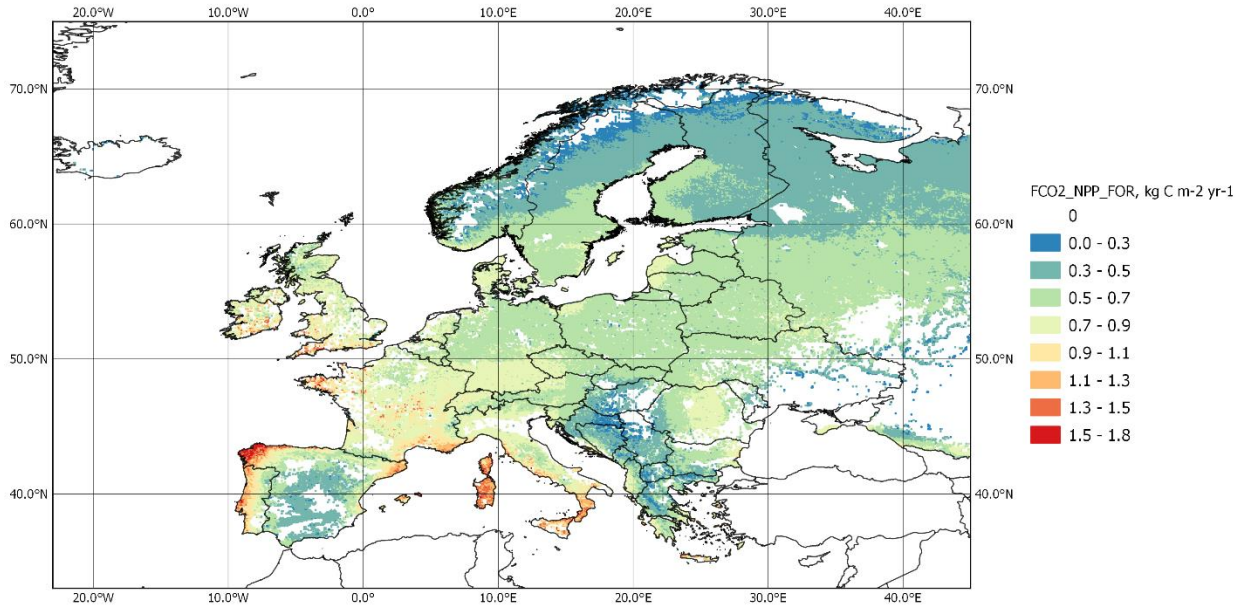


Figure 19 : Results from the G4M+FLAM model for the FCO2\_NPP\_FOR ( $\text{kg C m}^{-2} \text{ yr}^{-1}$ ) in 2020

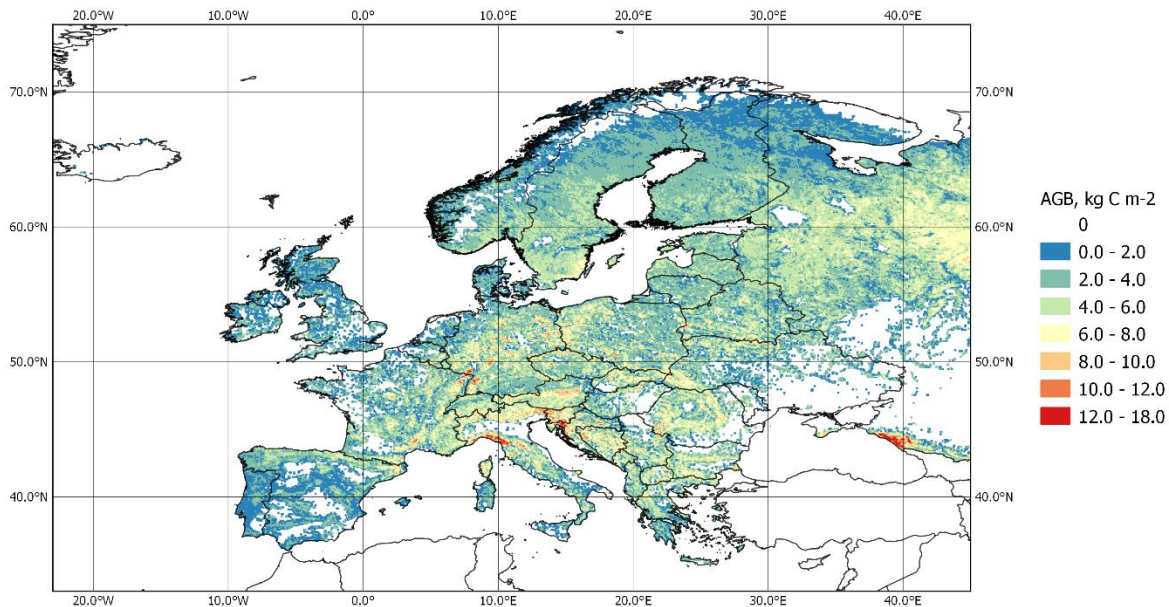
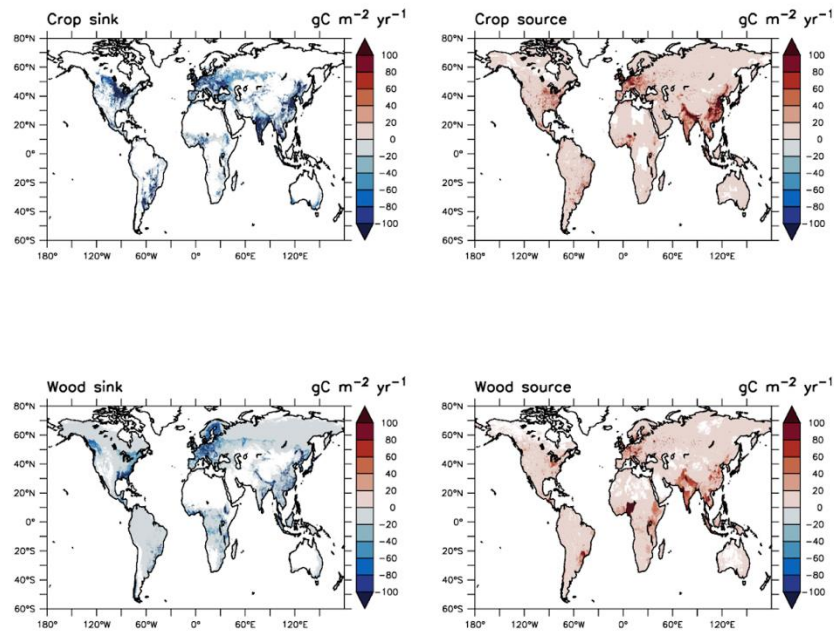


Figure 20 : Results from the G4M+FLAM model for the AGB ( $\text{kg C m}^{-2}$ ) in 2020.

## 5.10. Lateral Fluxes

Figure 21 illustrates two of the maps of the database. The maps show quite clearly that the location where the carbon is removed from the atmosphere by plant growth is not always the location in which the carbon is emitted due to the use of the product. Such a result could be very useful when comparing methods based on atmospheric inversions to those based on bottom-up inventories, as the observations used in the atmospheric inversions will take into account lateral transport of carbon but bottom-up inventories may not.



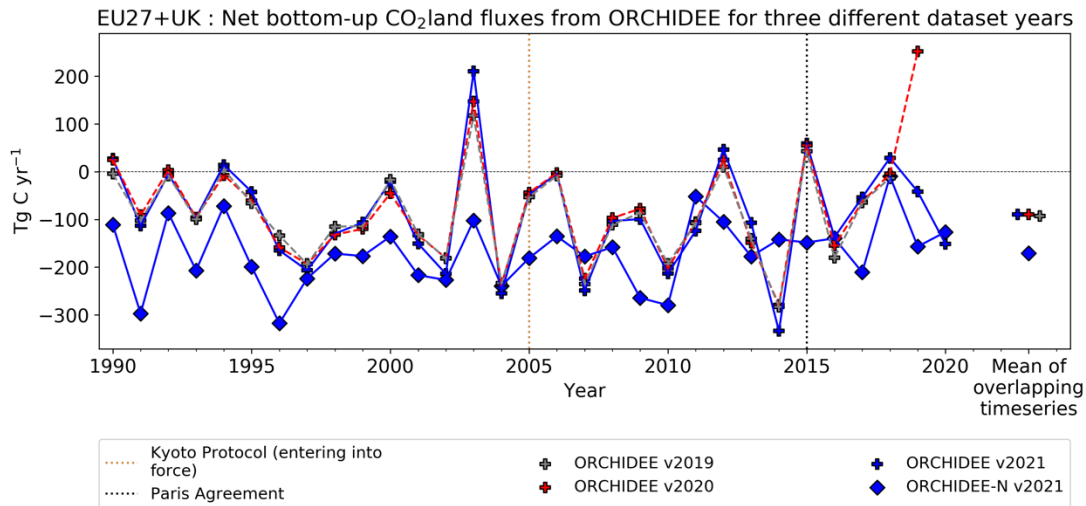
**Figure 21 : An example of lateral carbon fluxes showing the locations of the uptake of carbon by forests and croplands as well as the emissions related to the use of these products.**

## 5.11. ORCHIDEE

Figure 22 shows a comparison of the annual Net Biome Productivity (NBP) calculated from ORCHIDEE for the EU27+UK for the past three years of the VERIFY project. Both model versions ORC2/ORCHIDEE and ORC3/ORCHIDEE-N (the latter including a dynamic nitrogen cycle) are shown. Small changes can be seen between ORCHIDEEv2019 and ORCHIDEEv2021 due to the change in the meteorological forcing from CRUHAR to CRUERA5, but the resulting impacts on the NBP are relatively minor.

The year 2019 for run ORCHIDEEv2020 shows a very large difference compared to other years. After additional tests, this was determined to be related to the time axis on the meteorological forcing of CRUERA which was misaligned, leading to a decoupling of the diurnal cycles for some variables. This only affected a single year because ORCHIDEEv2020 used CRUERA for only 2018 and 2019; the issue occurred at the end of a full year of forcing data (2018) and propagated to the subsequent years, which in this case was only 2019. The issue has been fixed in the runs for the current deliverable, as can be seen by the more expected behavior of 2019 and 2020 for ORCHIDEEv2021.

The inclusion of the dynamic nitrogen cycle and its resulting limitation on photosynthetic activity leads to a stronger carbon sink in Figure 22 compared to the run without nitrogen. We are currently investigating the reasons for this.



CC BY VERIFY Project

**Figure 22 : A comparison of ORCHIDEE results for VERIFY runs from the past three years of the project. ORCHIDEE represents ORCHIDEE v2 (either 2.1 or 2.2), while ORCHIDEE-N represents ORC3 with a dynamic nitrogen cycle.**

## 6. Conclusions

The bottom-up simulations were designed to provide estimates of terrestrial carbon dioxide fluxes from natural and human-influenced ecosystems, including croplands, grasslands, and forests.

Major advances in model refinements this year included: FLUXCOM upgrading to v2.0 and improving the quality of the training data; ECOSSE significantly improving results through changes in data and model structure; EFISCEN-Space extending results to fifteen countries with spatially-explicit methods based on forest inventory data; CBM adding a projected simulation for the forest NBP in the year 2020 (previous results were only available through 2015); BLUE running at the original very high-resolution of the Hilda+ dataset (0.01 degrees); and ORCHIDEE including a model version with a dynamic nitrogen cycle.

In addition, new models have been added. This includes an effort to estimate bottom-up carbon dioxide fluxes from coastal ocean regions, which have been incorporated into top-down inversions in WP3; efforts to estimate lateral transport of carbon through rivers and trade flows, taking into account that where carbon is assimilated by plants is not always the location of where it is emitted by humans; and the participation of the CABLE-POP model to demonstrate how the VERIFY dynamic global vegetation model protocol can be adopted by other research groups to carry out a wider intercomparison.

Technical work remains to harmonize more of the forcing data used in the models. While land cover/land use data (Hilda+ dataset) and meteorological forcing products have been provided by VERIFY partners and are being used by several of the models, some additional work is still needed to ensure the widest-possible use of these data. In addition, several of the models simulate processes around the nitrogen cycle. Nitrogen datasets have been provided through VERIFY in 2021, but the work has not yet been widely adapted. The meteorological forcing will require significant attention in 2022. ECMWF, who produces ERA5-Land, has reported delays to the creation of ERA5-Land due to the Covid19 pandemic; originally scheduled to be complete at the end of 2020, completion is now projected by mid-2021. The years 1951-2020 are now currently available for download, and we are beginning to process the years which have not previously been treated.